University of Jordan.

Faculty of Graduate Studies

COMPOSITE COLUMNS OF SEMI-ENCASED SECTIONS

BY

JAMAL BAZLAMIT

SUPERVISOR

DR. YASSER HUNAITI

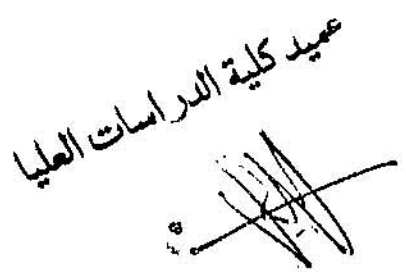

"Submitted in partial Fulfillment of the Requirements for the Degree of Master of Science in Civil Engineering,

Faculty of Graduate Studies

University of Jordan

Jan. , 1993

The examining Committee considers this thesis satisfactory and acceptable for the award of the degree of Master of Science in Civil Engineering.

Dr. Yasser Hunaiti (Supervisor)

(University of Jordan)

.....

Dr. Abdel Qader S. Najmi (Member)

(University of Jordan)

.....

Dr. Adel A. Tayem (Member)

(University of Jordan)

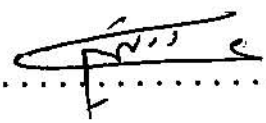

.....

ACKNOWLEDGEMENTS

This work was carried out under the supervisor of Dr. Hunaiti. Y., to whom I am grateful for his encouragement, guidance, useful suggestions and patience through out this study.

Tests were carried at the Heavy Structure Laboratory of Civil Engineering Department, at the University of Jordan, and I wish to thank the Department administration for providing all possible facilities.

The financial assistance of the Faculty of Graduate studies (H.& I. Mango Fund Committee) is gratefully acknowledged, for supporting the experimental part of this study.

The writer wishes to thank and acknowledge Hamdan, M., Riyalat, S., and Irshedat, H. for their help in computer programming and Qtaishat, T. for her help in typing the thesis.

TABLE OF CONTENTS

LIST OF TABLES

LIST OF FIGURES

NOTATION

A_c :Area of concrete.

A_s :Total cross-sectional area of steel.

B :Width of semi-encased section.

D :Depth of semi-encased section.

EI :Flexural rigidity of section.

e :Eccentricity of the load.

e_A :Eccentricity of the load at end A.

e_B :Eccentricity of the load at end B.

F_{cu} :28-day cube strength of concrete.

F_y :Specified yield strength of steel.

H :Depth of column section.

K_1 :Factor to take account of the discrepancy between the strength of the concrete in the column and that in a cube.

L :Length of the column.

L_{cr} :Critical length of the column.

L_e :Effective length of the column.

L^* :Length of the equivalent column in post buckling state used in CDC method.

M :Bending moment.

M_A :Applied end bending moment at end A.

M_B :Applied end bending moment at end B.

M_{cr} :Critical bending moment

M_i :Bending moment at node i.

M_o :Larger applied end moment.

M_u :Ultimate moment of resistance, when axial load equal zero.

$M_{u(p)}$:Ultimate moment of resistance, for axial load increment equal to P.

N_c :Failure loads obtained by CDC method.

N_e :Failure loads obtained experimentally.

N_n :Failure loads obtained by Newmark's technique.

N_t :Failure loads obtained theoretically.

N_u :Squash load of the column.

P :Axial load increment.

P_{cr} :Critical axial load.

P_u :Squash load of the column, same as N_u.

P^* :Resultant force of axial load and reaction at the end of the column.

R :Reaction of the beam-column at support.

t_f :Flange thickness

t_w :Web thickness

w_i :Deflection at node i of the equivalent column.

w_o :Deflection at left end of the equivalent column.

X :Distance from the left end of the column.

X_i :Distance at node i from the left end of the column.

α_c :concrete contribution factor.

β :End eccentricity ratio, i.e :β equal to the smaller end applied moment divided by the larger end applied moment.

γ :Angle of inclination of P^*.

ϵ :Strain

ϵ_u :Maximum allowable concrete compressive strain.

θ_i :Slope at node i.

θ_o :Initial slope at left end.

ϕ :Curvature.

ϕ_i :Curvature at node i along the CDC.

ϕ_0 :Curvature at left end of the CDC.

δ_e :Deflection obtained experimentally.

δ_{T1} :Deflection obtained theoretically, (K_1=0.83).

δ_{T2} :Deflection obtained theoretically, (K_1=0.67).

ABSTRACT

Many experimental and theoretical studies have been carried out to study the behavior of composite columns. On the other hand, little investigations were conducted on semi-encased composite columns.

In addition to the advantages of traditionally types of composite columns, the semi-encased composite columns offer high impact resistance, simplified beam-to-column connections as well as reduction or omittion of shuttering.

As a part of a general investigation on the behavior of semi-encased column sections, at the University of Jordan, theoretical and experimental works were carried out in this study. Ten columns were tested up to failure under eccentric axial load. The cross sectional area and the slenderness ratio were held constant.

The variable studied in this research program are the eccentricity of the applied load and the composite action in such column, or in other words, the effect of omitting the shear connectors on the behavior and the load carrying capacity are evaluated.

The maximum strength of the tested columns were obtained by deflection methods using Newmark's technique of numerical integration and the Column Deflection Curve method.

The validity of the analytical methods is examined by comparison with experimental tests, and it was found that there is a good agreement between experimental and theoretical values.

CHAPTER I

INTRODUCTION

1.1 General

By definition a composite steel-concrete column is a member with a cross-section consisting of a steel section (or sections) and concrete which act together to resist axial compression.

Until the 1950s, steel columns where usually encased in low-strength concrete primarily to provide fire protection. Modern design of composite columns makes use of both the strength and the fire protection resistance of concrete and therefore provide a more economical structure.

Composite construction has several advantages over the traditional reinforced concrete or steel structures: these include high strength-to-weight ratios (compared with reinforced concrete structure), structural integrity, durable finishes, dimensional stability and sound absorption.

1.2 Types of Composite Columns

The structural steel component in a composite column is limited in practice by current experience in design and construction. Only two common types of composite columns are in use: steel sections encased in concrete and hollow sections filled with concrete, Figure [1.1].

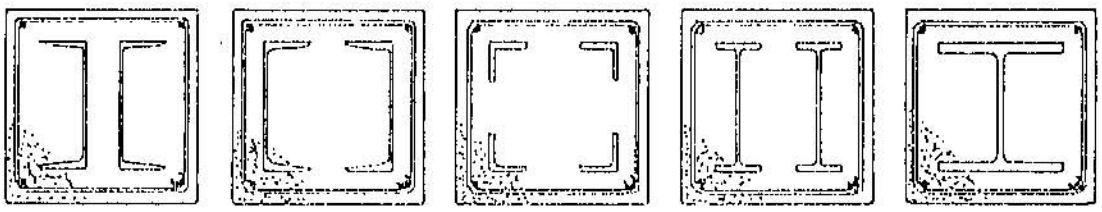

(a) Concrete-encased composite columns

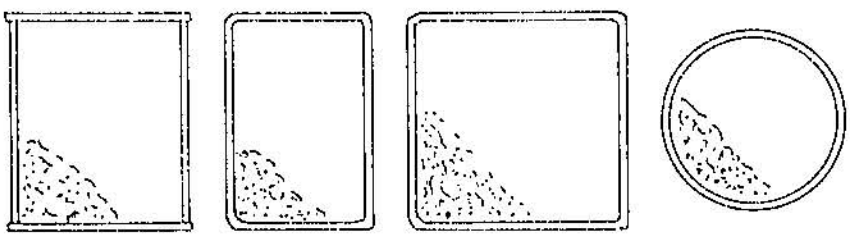

(b) Concrete-filled composite columns

Figure (1.1): Types of composite columns

In the case of concrete-encased composite columns, the structural steel component could be either one or more rolled steel sections which may be tied together. The concrete encasement enhances the behavior of the structural steel core by stiffening it, and so making it more effective against both local and overall buckling. The concrete encasement performs the additional function of fire resistance to the steel core. The main disadvantage of this type is that it requires a complete form work, furthermore, a reinforcement cage is required in order to prevent the concrete cover from spalling.

The concrete-filled composite columns have the advantage that they require no form work and no reinforcement. The most common steel sections used are the hollow rectangular and circular tubes. The main disadvantage of this type is that the concrete does not provide protection to the steel against fire, another disadvantage is the difficulty of beam-column connections.

A new type of composite column has recently been suggested for research and use. It consists of rolled I-section, semi encased with concrete around the web, Figure [1.2].

In this type considerable saving are achieved in time and material of construction, owing to the elimination of the steel ties in the column as well as the reduction in the form work.

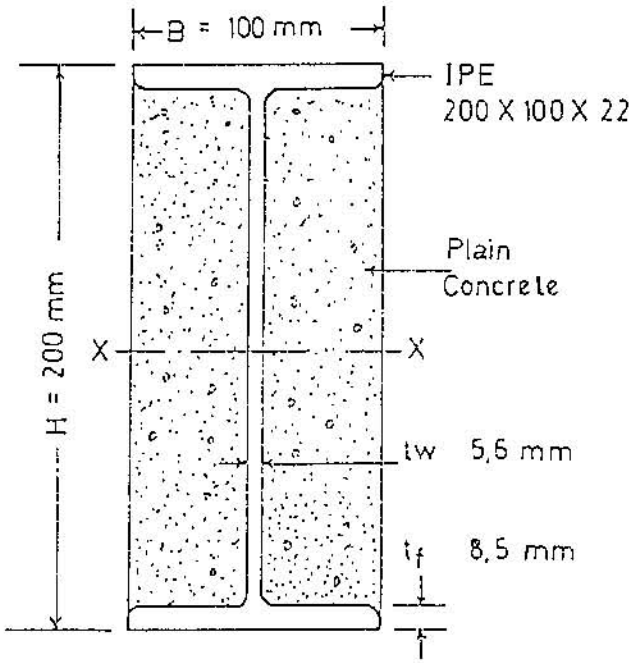

Figure (1.2): Semi-encased composite column

This research is conducted to investigate the behavior of the semi-encased composite columns.

1.3 Previous research

Steel-concrete composite columns have been in use since early this century. The concrete was a mix of low grade used originally as a fire protection to the structural steel section.

Early studies showed that the presence of the concrete encasement enhances the load carrying capacity of the steel sections also the encasement of concrete provides

restraint against both local and overall instability of structural steel core.

In 1905, the first recorded tests on built-up composite columns carried out by Emperger [1]. This early experimental investigation of the column behavior was confined to concentric loading only.

In the 1950s Faber [2], Stevens [3] and others carried out test on encased stanchions, to study the effect of the concrete encasement on the load carrying capacity. These studies had led to development of the cased-strut method of design which was incorporated in the 1959 edition of B.S 449.

In 1962 Jones and Rizk [1] carried out some tests on encased stanchions, both in field and laboratory to investigate the general behavior of composite column.

Later in 1967 a computer program was written by Basu to calculate the failure loads of pin ended composite columns of rectangular cross section having equal end eccentricities under the uniaxial bending [4].

In 1968 Furlong [5] carried out some tests on short concrete-filled tubes. In this study equations for stiffness and strength were developed and the result showed favorable agreement with test results.

Later on 1969, Knowles and Park [6] conducted a series of tests on steel tubes filled with concrete, loaded axially and eccentrically and covering a wide range of slenderness ratios.

Furthermore, fundamental research by Basu and Sommerville [7], and further work by Virdi and Dowling [8] led to the present design method of composite columns in the new British Standards [9]. This design method covers both cased-strut and concrete filled steel tubes, and also takes into account uniaxial as well as biaxial bending.

In 1981, Litzner and Crisinel [10] investigate the effect of residual stresses in steel sections on the carrying capacity of composite columns. The result was compared with that obtained for bare steel column.

In 1986, Dunberry, Leblance and Redwood [11] carried out some tests in which short rectangular steel columns filled with concrete are loaded to failure under axial load. In their study, the effect of the column strength was studied.

As part of a general investigation of the behavior of composite columns, theoretical and experimental works where carried out at the University of Jordan by Riyalat [12], Al-Hallie [13], Irshedat [14], Hamdan [15], Sawalha [16] and Asad [17] to compute the failure loads of pin-ended columns under uniaxial bending. In their calculation of failure loads,

Newmark's method of numerical integration and Column Deflection Curve were used.

From all previous investigations, the major findings could be summarized as follows:

1. Composite action between concrete and steel was confirmed.
2. The capacity of a composite column is affected by type of loading and dimensions of the column.
3. The difference between the experimental and theoretical failure loads was found to be reasonable.
4. The available design methods of composite columns proved to be safe and adequate.

In conclusion, the semi-encased sections have received little attention from the researchers, no investigations were recorded on this type of composite sections. Until recently an experimental research is conducted at University of Jordan by Hunaiti [18], in which ten columns of this type were tested under uniaxial loading to investigate the general behavior of this column.

1.4 Objective and Scope

Most of the previous research, both experimental and theoretical, had dealt mainly with concrete-encased and concrete-filled composite columns.

As a part of a general investigation on the behaviour

of semi-encased column sections, at the University of Jordan, theoretical and experimental works will be carried out in this study.

An experimental study was conducted on ten full scale columns of semi-encased sections. All specimens were tested under minor axis bending.

The variables studied in this research program were the eccentricity of the applied load and the composite action in such column, or in other words, the effect of omitting the shear connectors on the behavior and on the load carrying capacity was also evaluated.

The maximum strength of the tested columns are obtained by deflection methods using Newmark's technique of numerical integration and the Column Deflection Curve method.

CHAPTER II

THEORY AND ANALYSIS

2.1 General

All column problems can be approached from the standpoint of deflection. This isknown as the load-deflection approach. This attempts to solve the problem by tracing its load-deflection behavior throughout the entire range of loading up to failure.

Calculation of deflections in the elastic-plastic range are difficult in general, and numerical procedure are often necessary. Computer programs were developed at the University of Jordan by Riyalat [12] and Hamdan [15] to find the load carrying capacity of composite columns by Newmark's method and the Column Deflection Curve method (CDC). These programs are used in this study to calculate the ultimate loads of the tested columns.

2.2 Basic properties of composite columns

In order to study the behavior of composite columns, the following properties are derived for short composite columns, in which instability is ignored. In structural stability the term 'short column' refers to a compression member which can attain the ultimate load carrying capacity (maximum stresses of its components) with no sign of either local or overall buckling.

2.2.1 Squash load, Nu

Squash load, Nu, is defined as the ultimate short-term axial load for short column. The structural steel components of a short composite column yield before the attainment of the compressive strength of the concrete.

The load acting on the column section may be increased beyond that which causes the structural steel component to yield because the concrete encasement restrains the yielded steel part and prevents its buckling. The failure load of column section is attained when concrete reaches its maximum compressive strength, this load (referred as squash load) is given by:

$$Nu = As\ fy + K_1\ Ac\ fcu \qquad .....(2.1)$$

where:

- Ac : Total area of concrete;
- As : Total area of steel;
- fy : Yield strength of steel, and
- fcu : Compressive strength of concrete.
- K_1 : Factor to take account of the discrepancy between the strength of concrete in the column and that in a cube.

It should be mentioned that in computation of failure loads by numerical methods, no material partial safety factors are introduced for steel and concrete. Moreover, two values for

K_1 are used in this study, where the first one is 0.67 which specified by BS [9], the second is 0.83 and this value is recommended by ECCS [19] for experimental work.

2.2.2 Concrete Contribution Factor, α_c

The concrete contribution factor is a parameter (or factor) which indicates the proportion of the squash load carried by the concrete alone. This parameter is given by:

$$\alpha_c = \frac{K_1 \, Ac \, f_{cu}}{Nu} \quad \ldots\ldots\ldots (2.2)$$

where:

Ac, f_{cu}, K_1 and Nu are as defined before.

2.2.3 Ultimate Moment of Resistance, M_u

The ultimate moment of resistance; Mu, (when axial load equal to zero) of a column section is determined by considering equilibrium across a fully plastic section. The calculation of the equilibrium condition is based on the standard practice of assuming rectangular stress blocks in both concrete and steel.

At failure, it is a normal practice to assume that the steel reached its yield stress both in tension and compression, and concrete in the compression side reaches its ultimate compressive strength, while the concrete in the

tension zone is cracked and neglected.

The position of the neutral axis in the section is determined such that compression forces are equal to tension forces, and then the bending moment is calculated.

The derivation of ultimate moment of resistance for a semi-encased-composite column bending about minor axis is given in Appendix A [18].

2.3 Design Methods for the Composite Columns

Steel-concrete composite columns have been used in various forms. It is only in the last few years that methods of design based on extensive theoretical and experimental work have become available for such columns.

The cased - strut method can be described as the oldest and simplest one for design of composite columns. It is based on little research and its load prediction was over conservative when compared to test results of composite columns [20].

Several theoretical studies and experimental investigations on the behavior of composite columns have been carried out since the 1960's [4,11,5,10,3]. The results of which have been incorporated in the British Standards BS 5400: part 5 [9], and also in the recommendations of the European

Convention for Constructional steelwork for the design of composite structures [19]. These design methods are only applicable to filled and encased composite columns.

2.4 Numerical Methods for Calculating Ultimate Loads

Many analytical methods have been used in generating the interaction curves of composite columns. One feature common to all of them, is that, it is first necessary to obtain the moment-curvature relations of the cross section as a function of the axial load. This known as the family of M-ϕ-P curves. The shape of these curves is dependent on the material stress-strain, and the shape of the cross section.

2.4.1 Moment-Curvature-Thrust Relations

For a given combination of axial force and bending moment acting on section, there exist a unique value of curvature. The M-ϕ-P data characterizes the behavior of the column with no buckling effect. It is the fundamental information that defines the required stress distribution and magnitude necessary for equilibrium, for a given strain distribution.

The M-ϕ-P relationship, in the case of uniaxial bending, involves 4 quantities; axial load, moment, distance of neutral axis and the curvature.

Values of ϕ are assumed, the distance of the neutral axis is varied between specific limits. For each position of neutral axis, strain, stress, and forces are computed. Summation over the section are carried out for the axial load and the moment.

Thus, for different locations of neutral axis, sets of values of ϕ, axial force and bending moment are obtained. In order to obtain M-ϕ values for specific value of P, linear interpolation is used. Figures [2.1-2.2] show the M-ϕ curves for a semi-encased composite column section bending about minor axis. M-ϕ values in Figure [2.1] are computed using a value of 0.83 for K_1 while in Figure [2.2] the value of K_1 was 0.67. It should be mentioned here that the values of M_u in Figures [2.1-2.2], are as computed from the computer program.

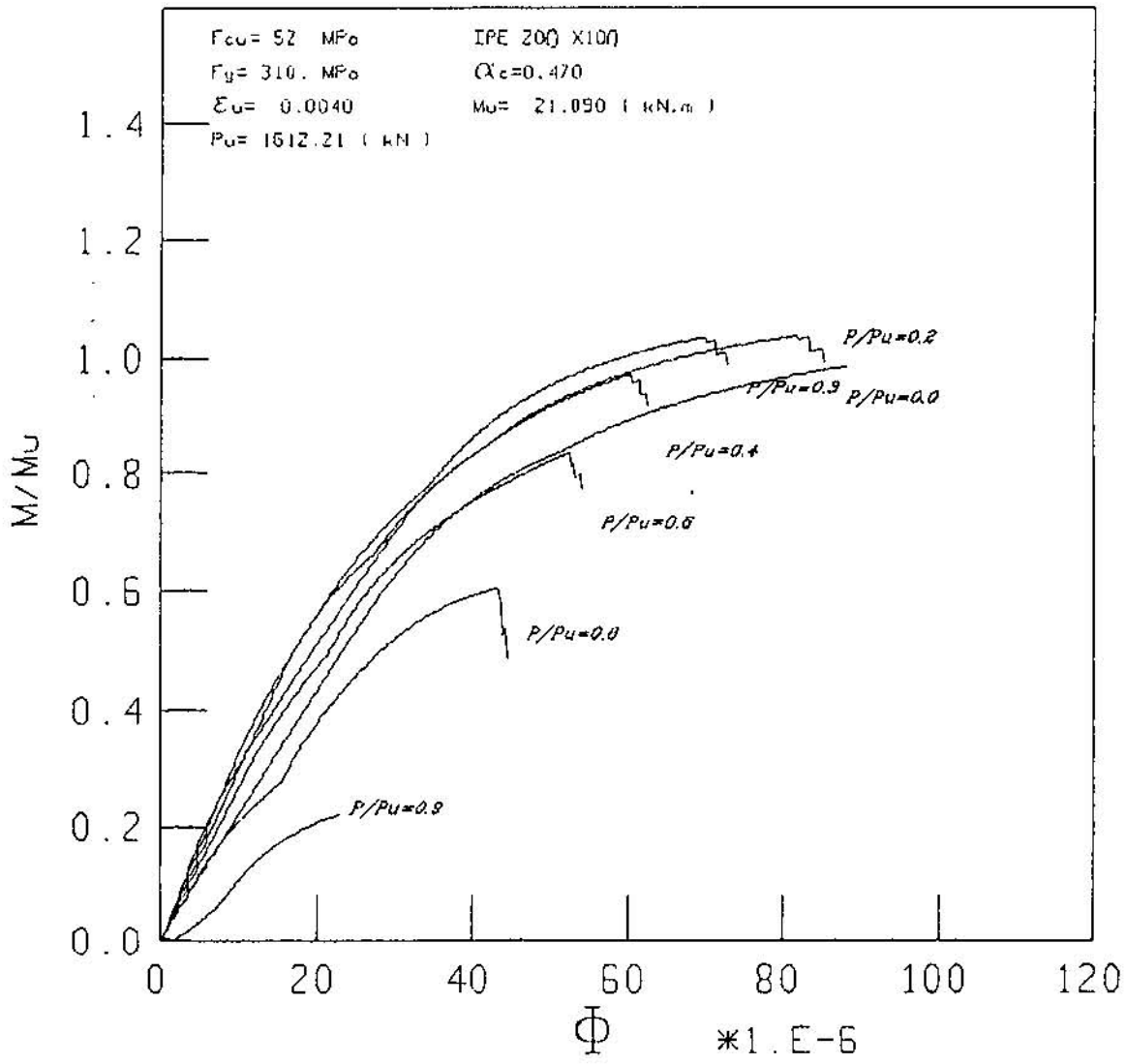

FIG. (2.1) : MOMENT-CURVATURE-THRUST CURVES FOR IPE SEMI - ENCASED COLUMN UNDER UNIAXIAL BENDING ABOUT MINOR AXIS

$K_1 = 0.83$

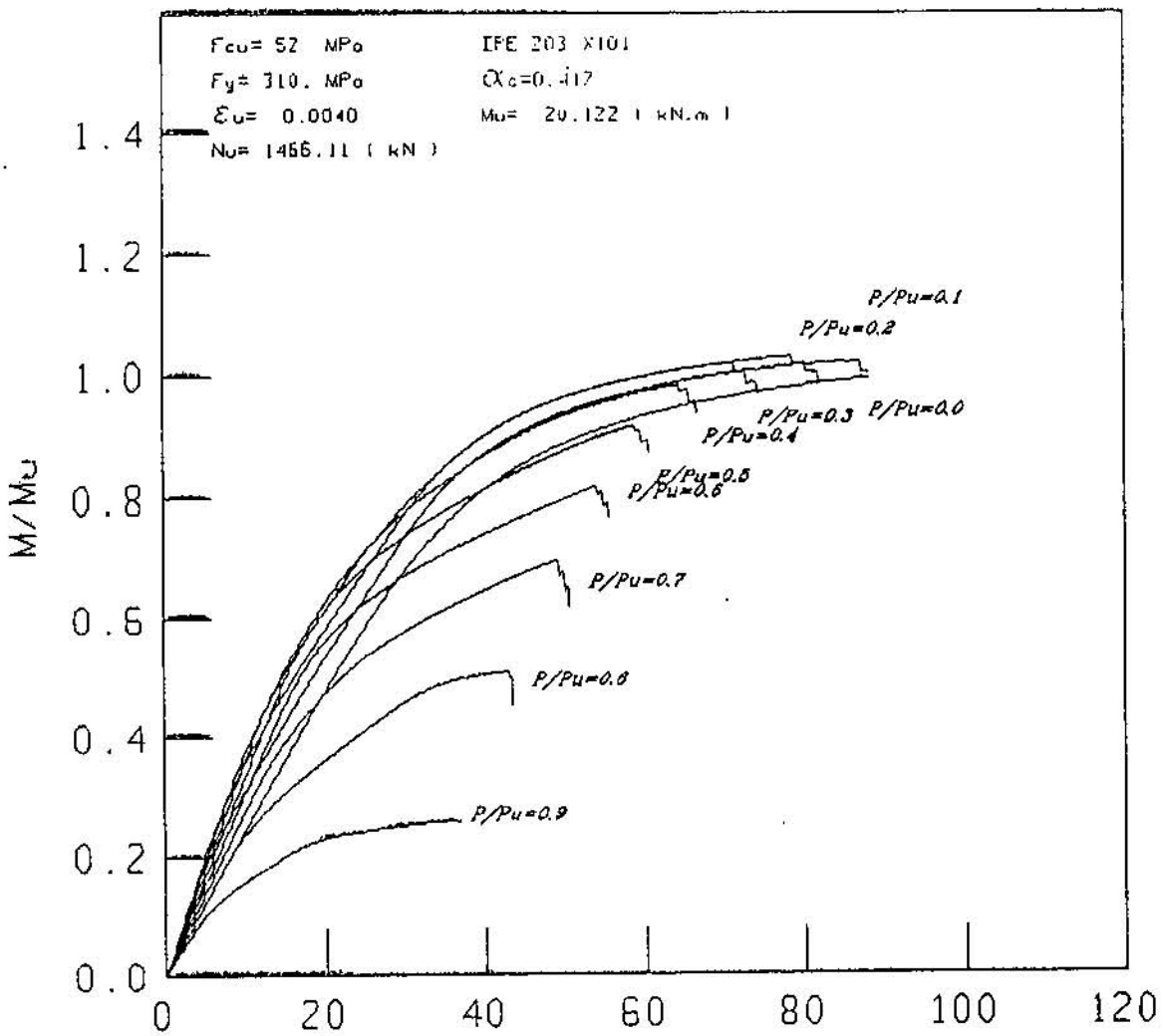

FIG. (2.2) : MOMENT-CURVATURE-THRUST CURVES FOR IPE SEMI - ENCASED COLUMN UNDER UNIAXIAL BENDING ABOUT MINOR AXIS

$K_1 = 0.67$

2.4.2 Computation of Failure Loads Using Newmark's Method of Numerical integration

This method can be used to determine the maximum value of end eccentricity, e,that a given column could sustain for specific values of eccentricity, column length and axial load.

In this method, for any given eccentricity ratio, the critical combinations of end moment and axial load can be determined for various lengths of a column and then the interaction curves can be constructed.

The outline of the scheme of computation of a failure load for a slender column in uniaxial bending is given below:

1- Section dimensions, material properties, column length and eccentricity ratio are defined.

2- $M-\phi$ values for a specific axial load are calculated and stored.

3- Critical length for the axial load is computed from the following equation

$$L_{cr} = \pi \sqrt{EI/P} \quad \text{.....(2.3)}$$

where

EI = Initial slope of $M-\phi$ curve.

P = Axial load increment.

4- If the length of the column is greater than the critical length, the analysis is terminated.

5- The larger end moment is assumed to be 0.005 M_u.

6- Column height is divided into (n) discrete intervals of length (Δx).

7- Initial deflections is assumed at each node point.

8- Bending moments at the node points are computed due to the assumed deflection and end applied loads.

9- Based on the node moments, and by interpolation from the M-ϕ curve, curvature distributions are computed.

10-The curvature is integrated twice to compute the new deflected shape.

11-The assumed values for deflection in step 7 is replaced by the new calculated ones in step 10, steps 7 to 11 are repeated until convergence is obtained to the desired accuracy.

12-If equilibrium is possible, the end moment is increased by 0.005 M_u and steps 6 to 11 are repeated.

13-If equilibrium is not possible, the column can be regarded as having failed due to critical end moments. The current value of the end bending moment is taken as the critical one.

A simplified flow chart for this method is given in Figure [2.3]. The interaction curves obtained by the current method are presented in Figures [2.4-2.5] for the same column, and considering K_1 as 0.83 and 0.67 respectively. It should be mentioned here that the values of M_u in Figures [2.4-2.5], are as computed from the computer program.

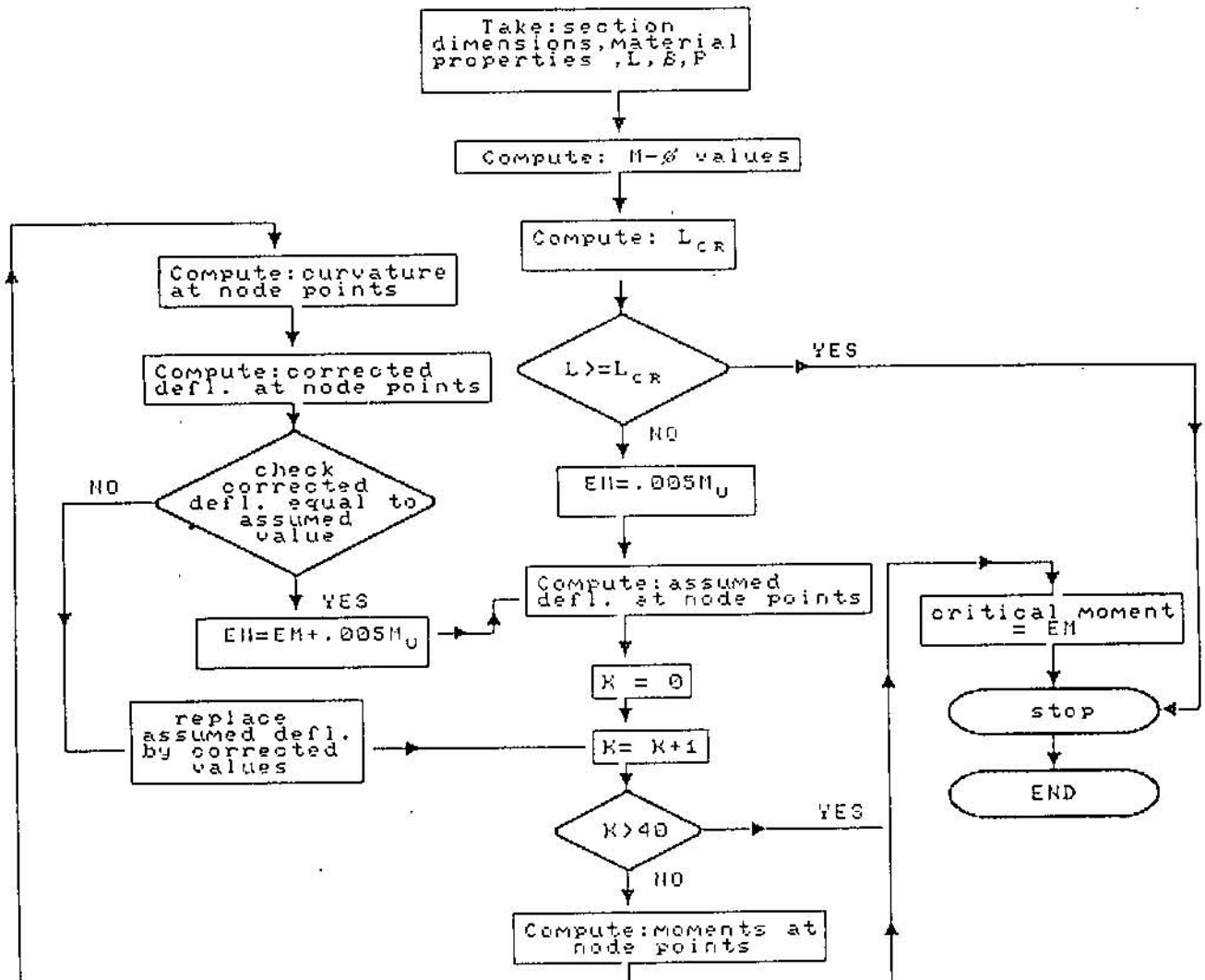

Figure (2.3): Flow-chart for Newmark's method of numerical integration.

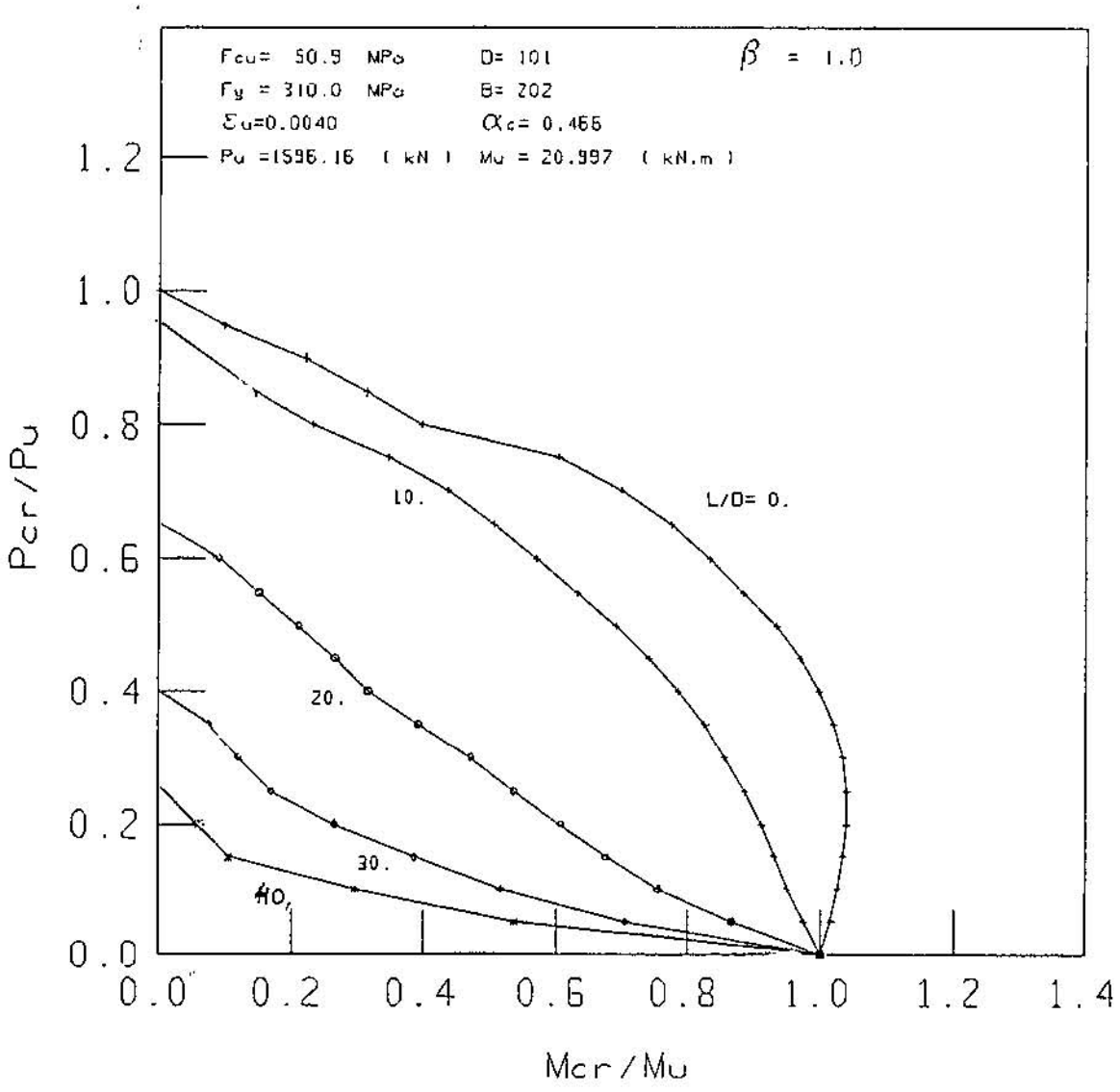

FIG. (2.4): ULTIMATE STRENGTH INTERACTION CURVES FOR IPE SEMI - ENCASED COLUMN UNDER UNIAXIAL BENDING ABOUT MINOR AXIS

** USING NEWMARK METHOD

$K_1 = 0.83$

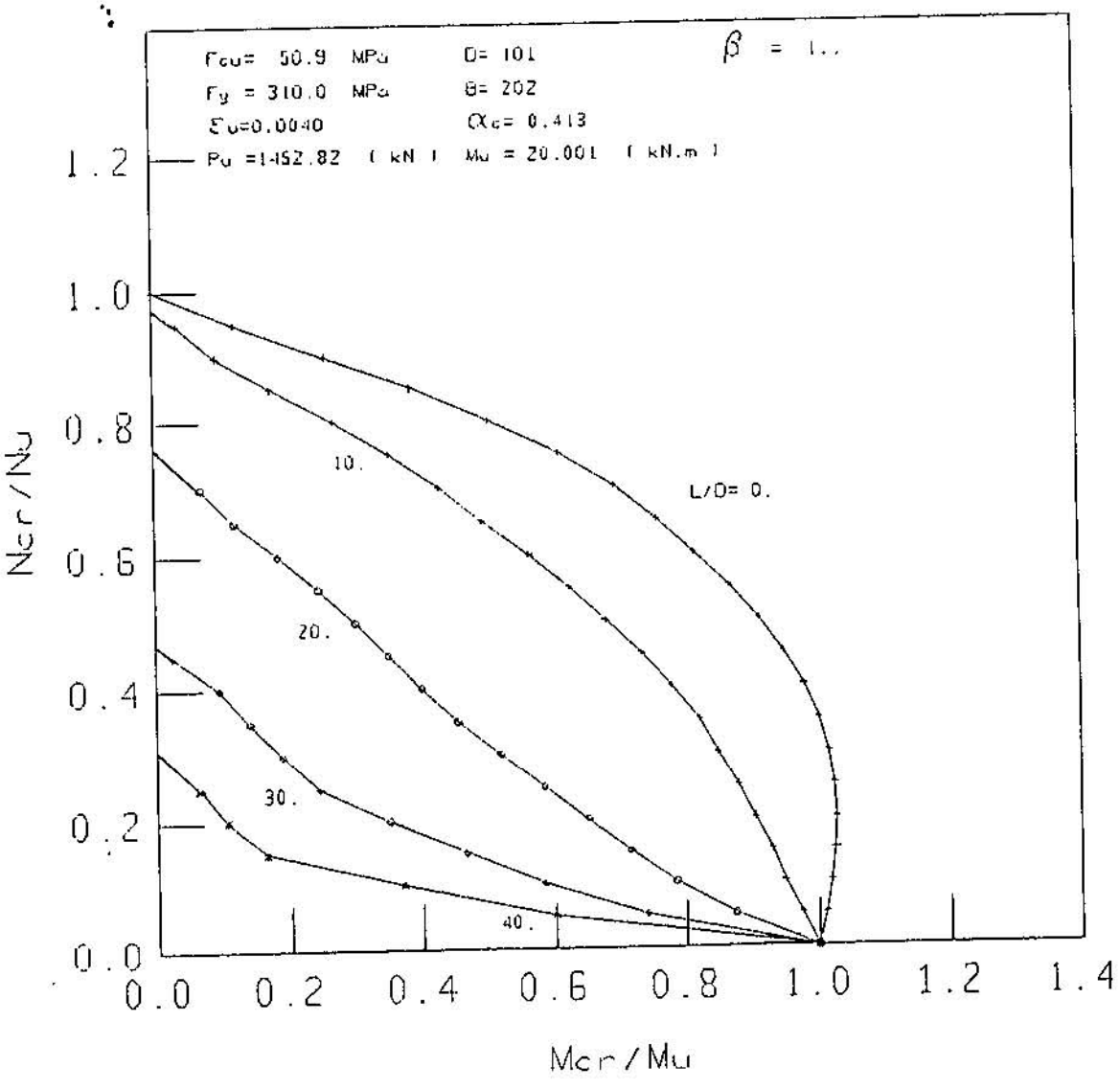

FIG. (2.5) : ULTIMATE STRENGTH INTERACTION CURVES FOR IPE SEMI - ENCASED COLUMN UNDER UNIAXIAL BENDING ABOUT MINOR AXIS

** USING NEWMARK METHOD

$K_1 = 0.67$

2.4.3 Computation of Failure Loads Using Column Deflection Curve Method

The CDC approach is employed in recent years to give solutions to various beam-column problems [15]. The method is based on the idea that for a given beam-column with end moments, an equivalent column exists.

Any beam-column with end forces P, M_a and M_b is represented by an equivalent column with axial force, P^*, a given length L^*, and an applied end rotation, as can be seen in Figure [2.6].

A portion of the equivalent column represents the deflected shape of the actual beam-column, some other portions of the same equivalent column represents the deflected shape of another beam-column as can be seen in Figure [2.7].

The solution for a given beam-column with length, L, and applied axial load, P, mainly starts by assuming end rotation values, and for these values, the equivalent column is computed, then the actual beam-column is allocated on the equivalent one.

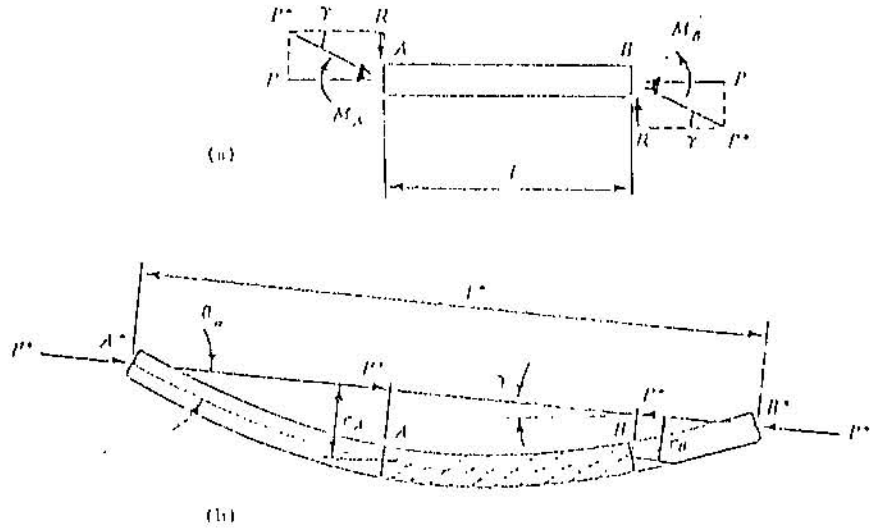

Figure (2.6): Equivalent column

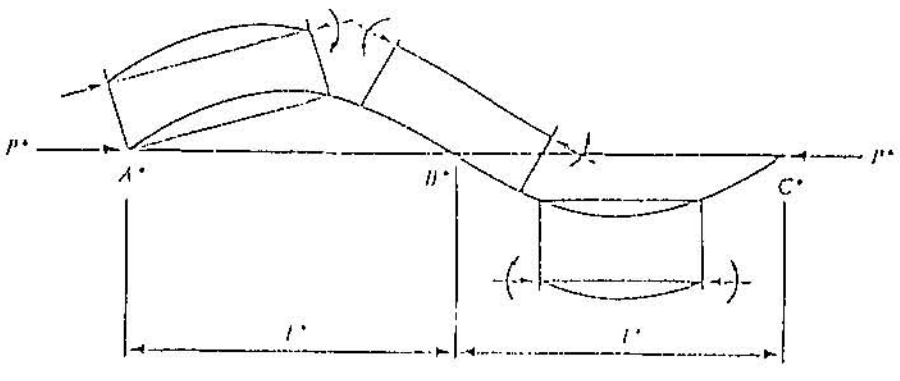

Figure (2.7): Beam-column under various loading conditions

The steps involved in implementation of the CDC method are as follows:

1- Section dimensions, material properties, eccentricity ratio, column length and axial load are defined.

2- M-ϕ values for the axial load are computed and stored.

3- An initial value for end rotation Θ_0 is assumed (in this study, this value is assumed to be 0.005 rad).

4- Equivalent column length is computed for this load increment and Θ_0 value and then CDC is constructed.

The numerical computation procedure for CDC or L^* is now explained with the aid of Figure [2.8] which shows a portion of a CDC near the end x = 0.0. Computation starts from the left end of the column at which deflection w_0 = 0.0, curvature ϕ_0=0.0 and M_0=0.0. The deflection w_i, Θ_i, ϕ_i at i-ith point x_i on the column are successively computed from the following equations:

$$W_i = W_{i-1} + \Theta_{i-1}(X_i - X_{i-1}) - 0.5\,\phi_{i-1}(X_i - X_{i-1})^2 \quad \ldots\ldots\ldots (2.4)$$

$$M_i = P^* W_i \quad \ldots\ldots\ldots (2.5)$$

$$\phi_i = f(M_i, P^*) \quad \ldots\ldots\ldots (2.6)$$

$$\Theta_i = \Theta_{i-1} + \phi_i (X_i - X_{i-1}) \quad \ldots\ldots\ldots (2.7)$$

For the purpose of computation of L^*, the procedure is repeated for every discrete point until the slope becomes zero or negative, while when constructing the CDC, the procedure is repeated for every discrete point on the imaginary column length L^*.

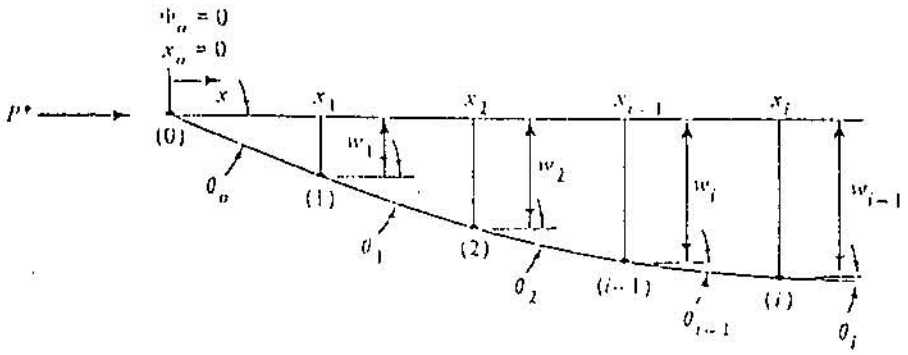

Figure (2.8): Numerical integration for CDC method

5- The beam-column is now allocated on the CDC, as can be seen in Figure [2.7] to compute and store for this applied end rotation Θ_o and axial load, the:

   a) End moment for the beam-column.

   b) End rotation for the beam-column.

6- Steps 4 to 5 are repeated for all other specified end rotations.

7- Critical maximum end bending moment and rotation are computed and stored from all the previously computed values.

A simplified flow chart for this method is given in Figure [2.9]. Interaction curves generated by this method are presented in Figures [2.10,2.11] for the same column, and

considering K_1 as 0.83 and 0.67 respectively. It should be mentioned here that the values of M_u in Figures [2.10-2.11], are as computed from the computer program.

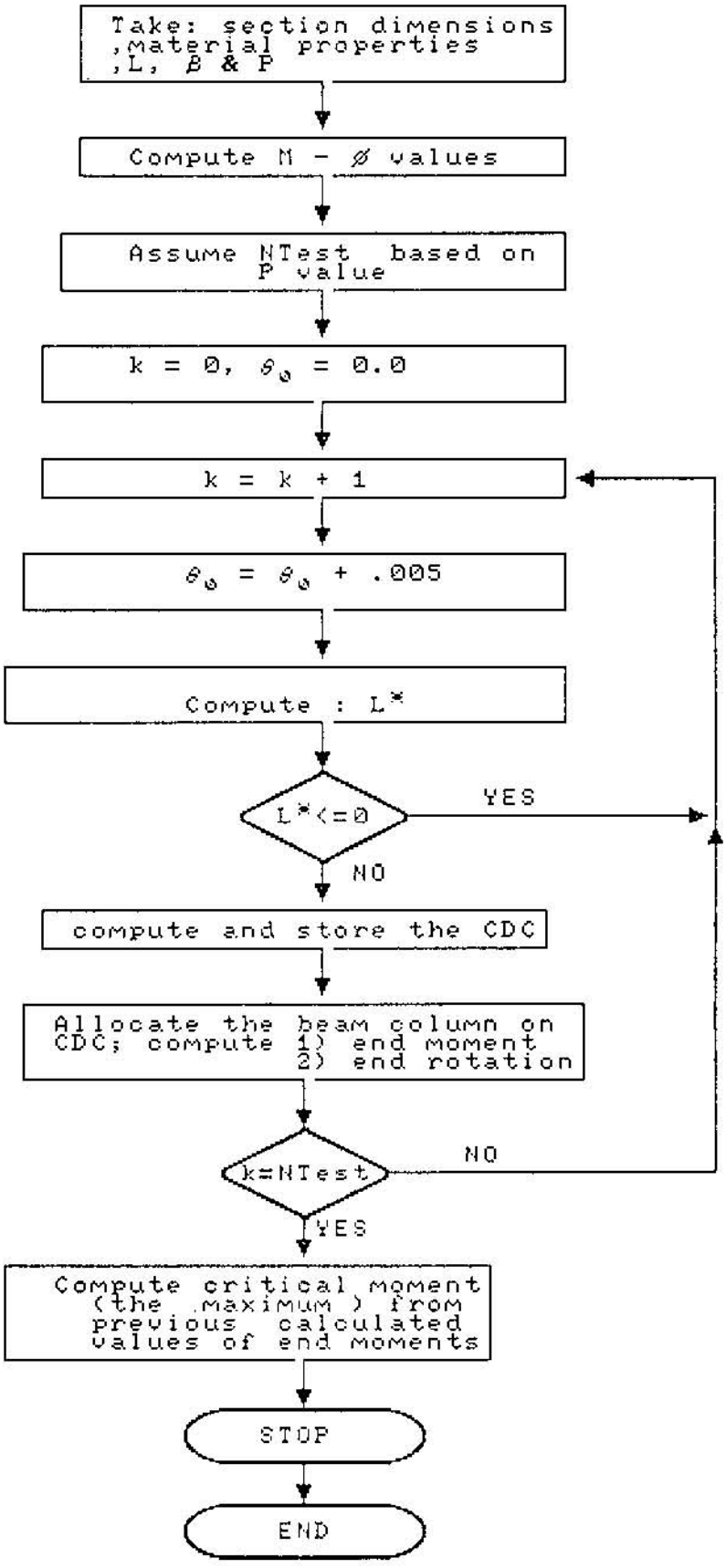

Figure (2.9): Flow-chart for Column Deflection Curve method

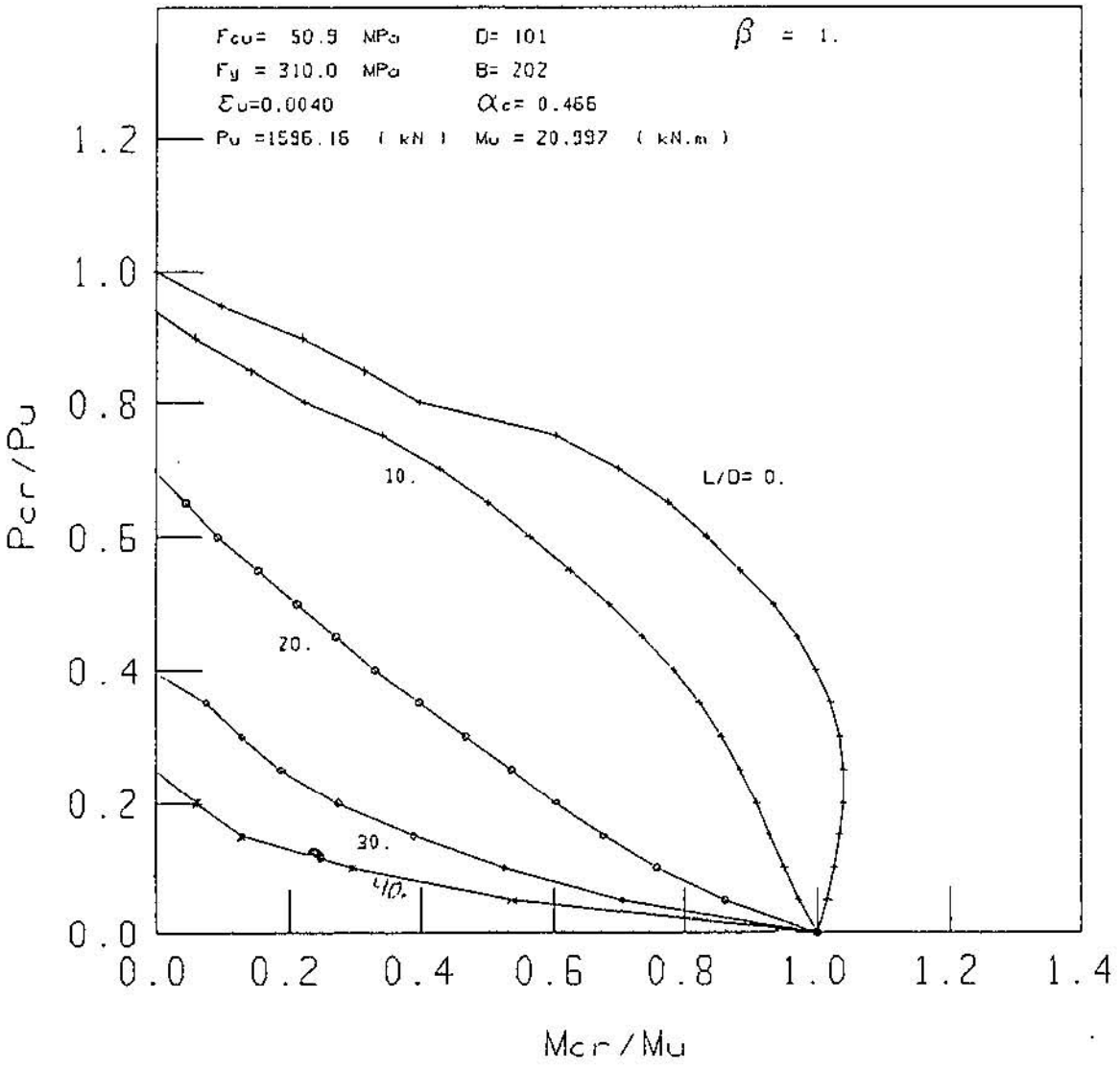

FIG. (2.10) : ULTIMATE STRENGTH INTERACTION CURVES FOR IPE SEMI - ENCASED COLUMN UNDER UNIAXIAL BENDING ABOUT MINOR AXIS

** USING C D C METHOD

$K_1 = 0.83$

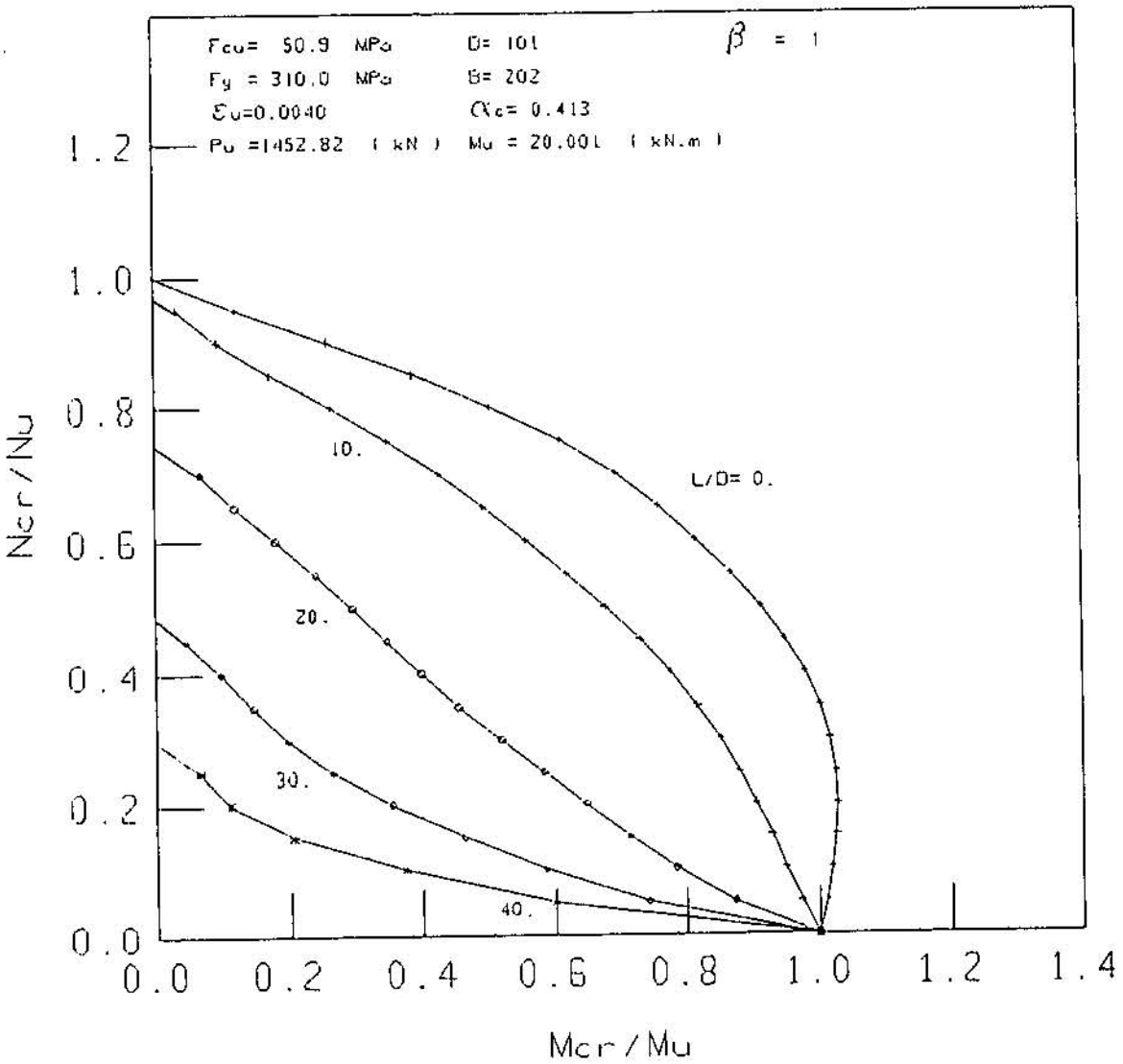

FIG. (2:11) : ULTIMATE STRENGTH INTERACTION CURVES FOR IPE SEMI - ENCASED COLUMN UNDER UNIAXIAL BENDING ABOUT MINOR AXIS

** USING C D C METHOD

$K_1 = 0.67$

CHAPTER III

EXPERIMENTAL PROGRAM

3.1 General

The semi-encased column sections have received little attention by the researchers.

In order to study the behavior of such column under load, tests were carried out on ten large-scale columns bending about minor axis. The variables studied in this research program are the eccentricity of the applied load and the effect of omitting the shear connectors on the behavior and on the load carrying capacity was evaluated.

3.2 Test Rig

Full scale tests on semi-encased composite columns were carried out at the University of Jordan. The capacity of the test rig used is 400 kN. Figure [3.1] shows the basic elements of the test rig.

The loading system consists of a hydraulic jack with circular end plate of 170 mm diameter and 25 mm thickness through which the load is applied.

The control panel is capable of providing data such as the applied load and displacements and plotting of the load-displacement of the tested column.

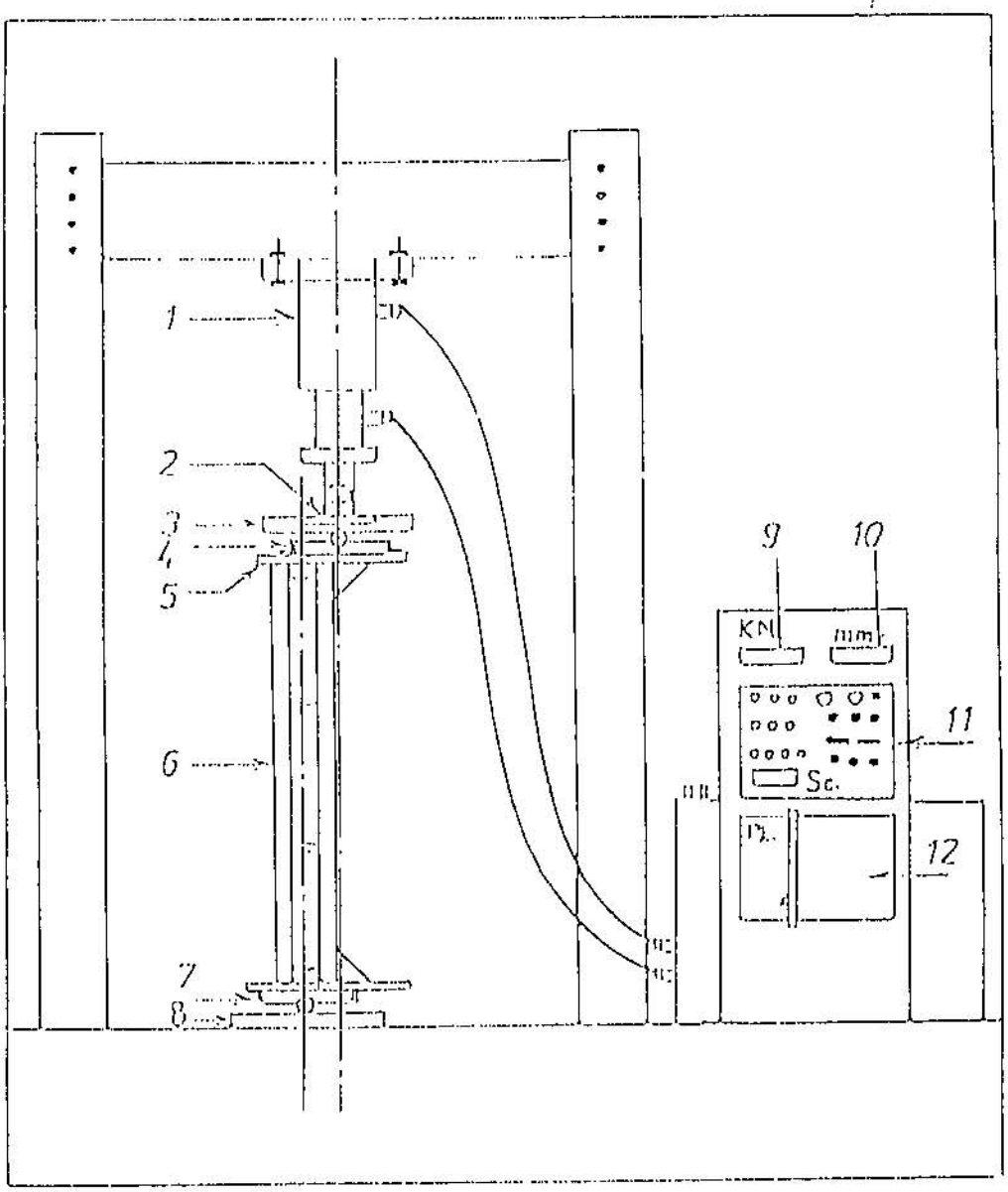

1. Hydraulic jack of 400 KN capacity.
2. Circular end plate of the jack.
3. Upper exterior loading plate.
4. Upper interior loading plate.
5. Specimen end plate.
6. Test specimen.
7. Lower interior loading plate.
8. Lower exterior loading plate.
9. Applied load indicator.
10. Vertical deflection indicator.
11. Operating panel.
12. Load deflection plotter.

Figure (3.1): Test Rig

The loading was applied to the column by means of a pair of loading plates, of 50 mm thickness, at each end of the column specimen. A cylindrical groove of 172 mm diameter and 25 mm depth, was made in the upper exterior loading plate such that the circular end plate of the jack can go through this groove before loading stage.

In between the loading plates, a circular bar of 200 mm length and 50 mm diameter was welded on the center line of the exterior plates. The lower exterior plate is fixed to the ground.

The interior end loading plates were placed near the column ends and to which the column end plates were bolted, enabled the columns to be accurately fixed to the thick loading plates with a high degree of accuracy in applying the load at the required eccentricities. A cylindrical groove of 50 mm diameter and 15 mm depth was made along the center line of the interior loading plates.

The interior loading plates were placed at the required eccentricity on each end plate of the column by means of two angles welded to the end plates of the column, then bolts of 10 mm diameter were used to fix these interior loading plates to the welded angles.

A ply of hard rubber of 3 mm thickness was placed between the interior loading plates and the end plates of the

column, to eliminate any fabrication errors. Details of upper and lower end supports are given in Figures [3.2,3.3,3.4,3.5].

A protecting frame (shown in Figure 3.6) was fabricated and erected under the test rig with the intention of fullfilling the following purposes:

1. Providing the facility of a proper installation of column specimen.
2. Providing the safety requirements while testing and after releasing the load.
3. Accommodating the specimen to the required eccentricity (a rail was designed at the base of the protecting frame in which the lower loading plate was placed).
4. Placing the dial gauges at specified locations.

The protecting frame was fixed to the ground by means of six tie-rods of 22 mm diameter.

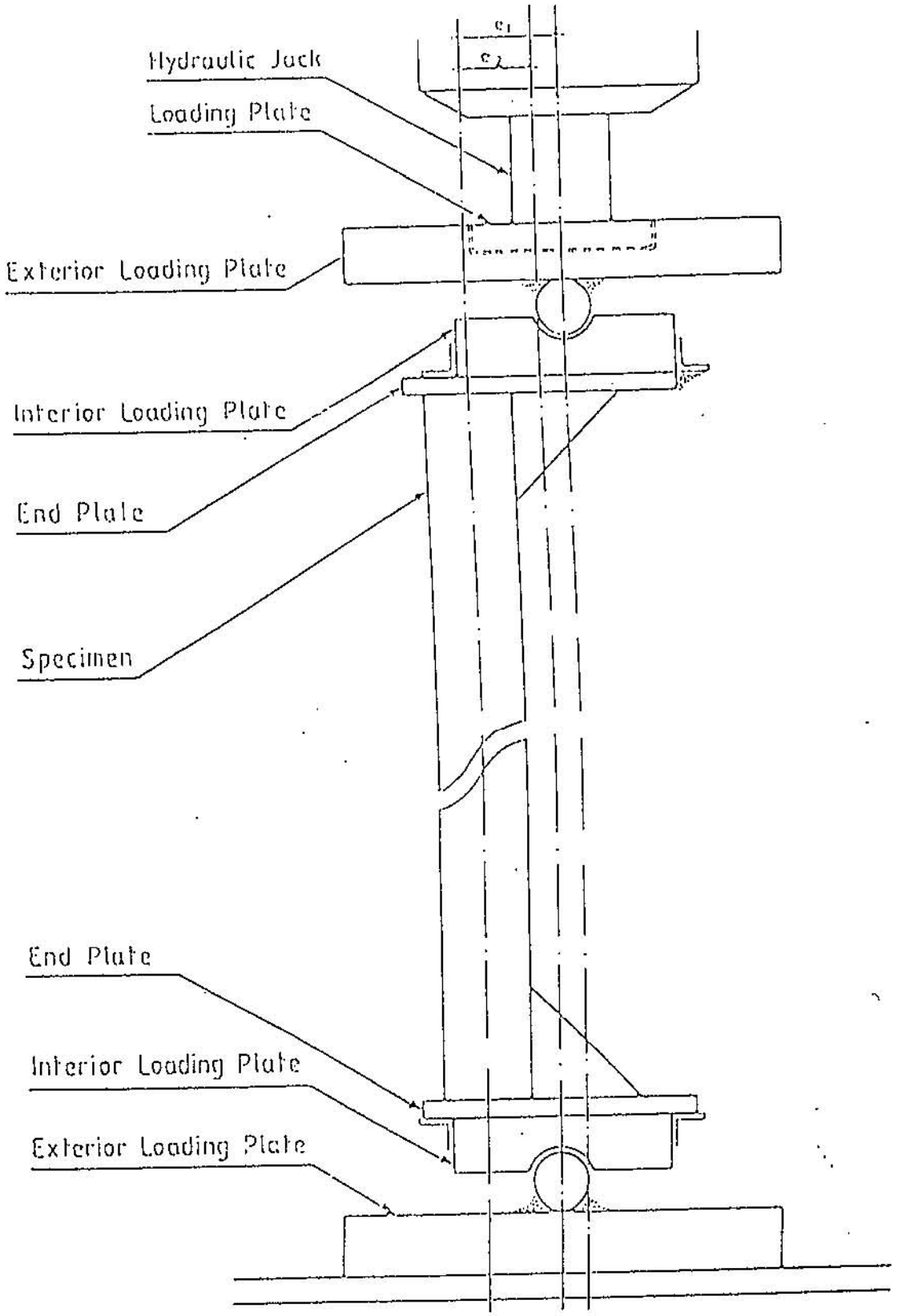

Figure (3.2): Test set-up

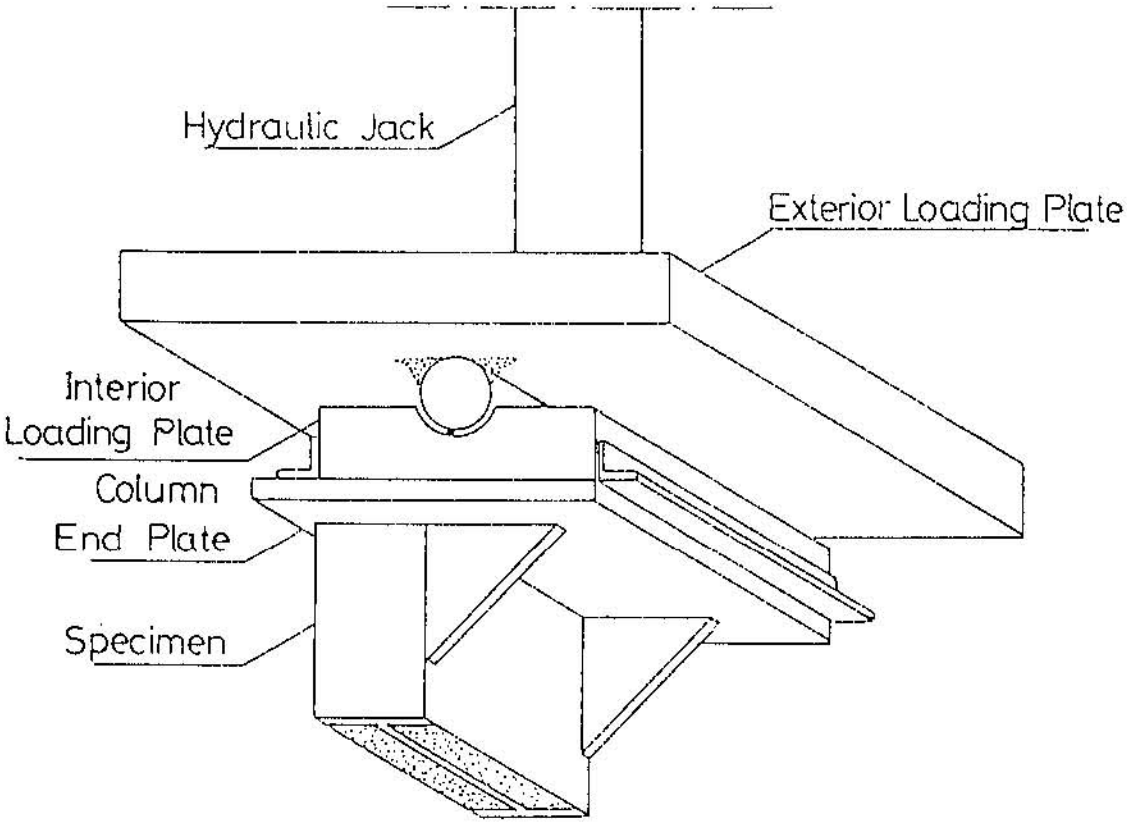

Figure (3.3): Details of upper end support

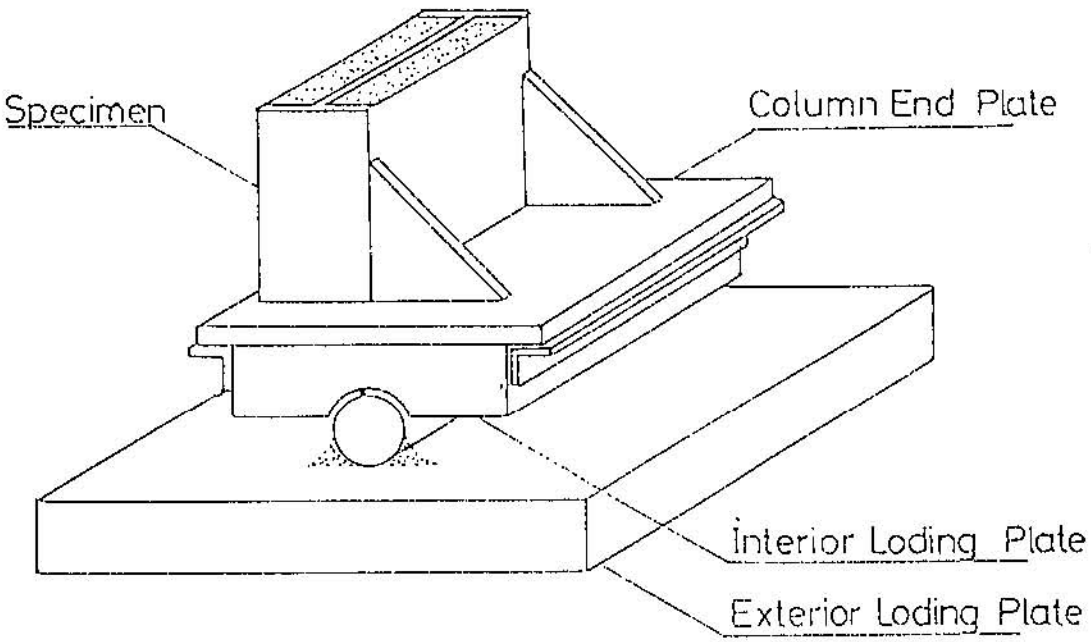

Figure (3.4): Details of lower end support

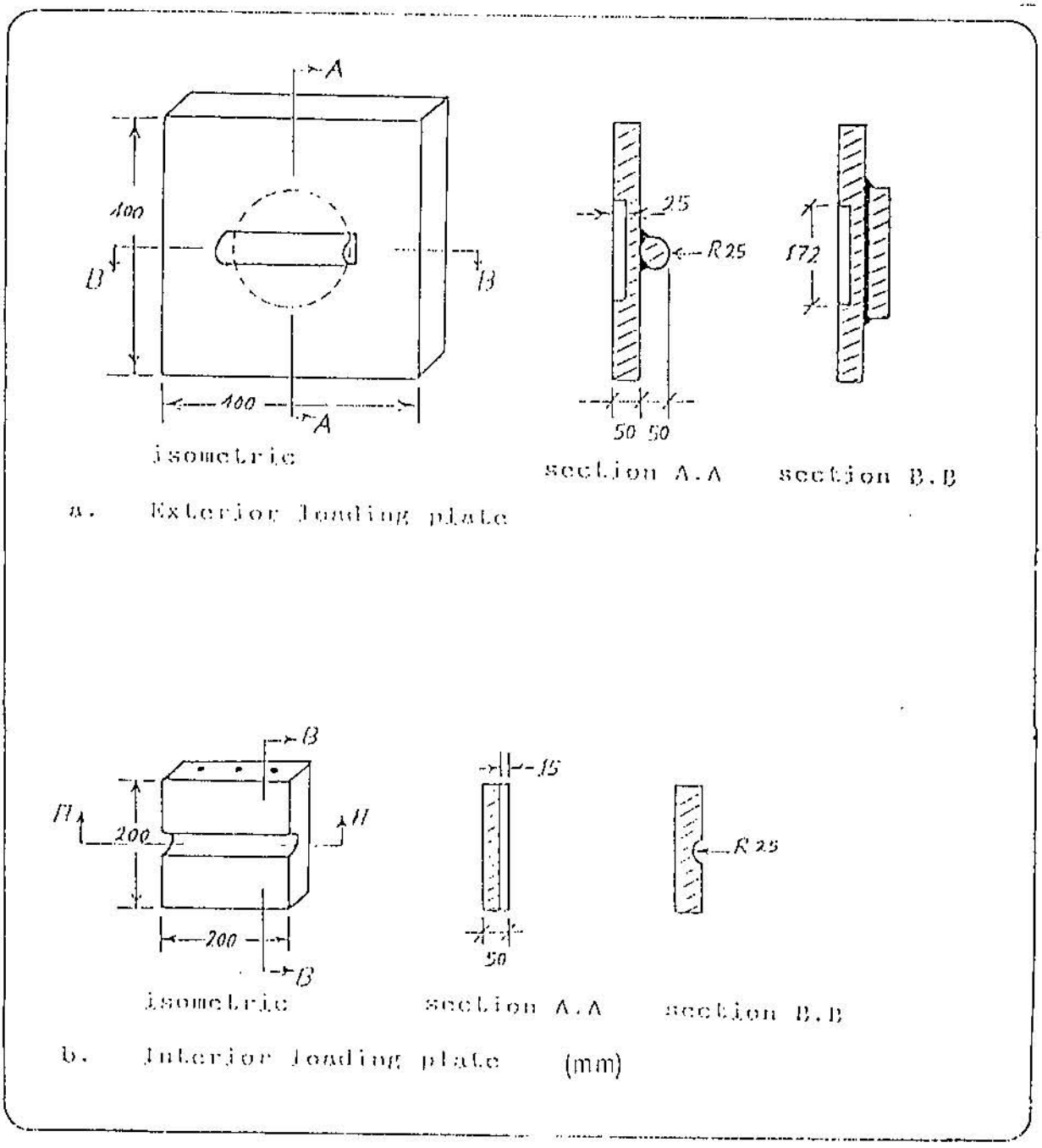

Figure (3.5): Details of loading plates

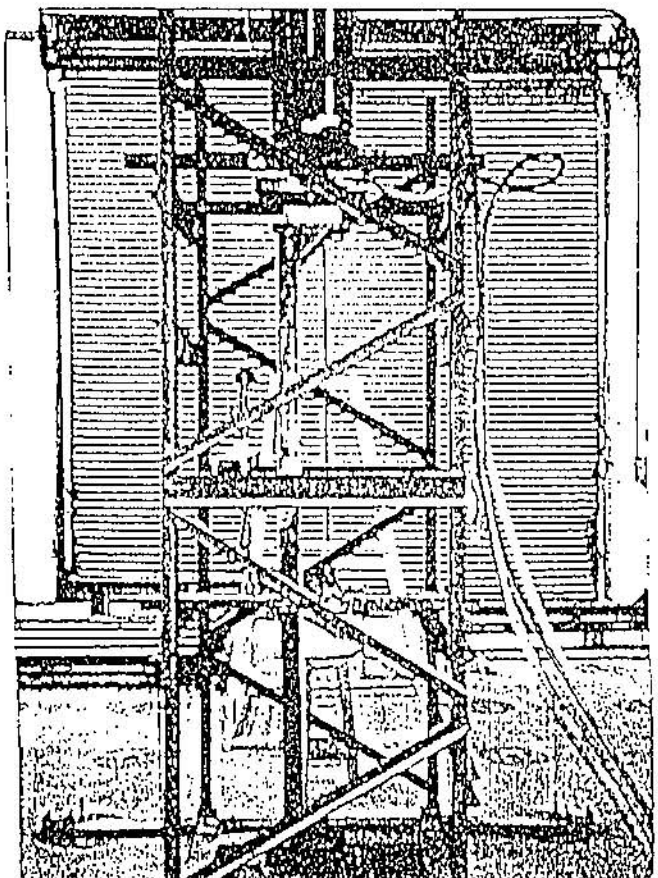

Figure (3.6): A test specimen placed in the test rig

3.3 Test Specimens

Ten columns were tested under eccentric loading, bending about minor axis and end eccentricity ratio equal to one. Figure [3.6] shows a test specimen placed in the test rig.

3.3.1 Details of the columns

The eccentricity of the load and dimensions of the tested columns were limited by the load-carrying capacity of the available laboratory facilities. All columns tested were of the same cross section shown in Figure [3.7]. IPE 200x100x22 steel sections, 2250 mm long, were selected for study due to the load and height limitation of the 400 kN MFL prüf systeme testing machine available.

Two end plates of 15 mm thickness were welded at the column ends. These plates were extended out of the column depth to accommodate the applied eccentric load within their dimensions.

Triangular stiffening plates of 10 mm thickness were welded to column end plates to ensure that premature failure would not occur as a result of local failure at the column ends. Figure [3.8] shows the column end with the extended end plates and stiffening triangular plates.

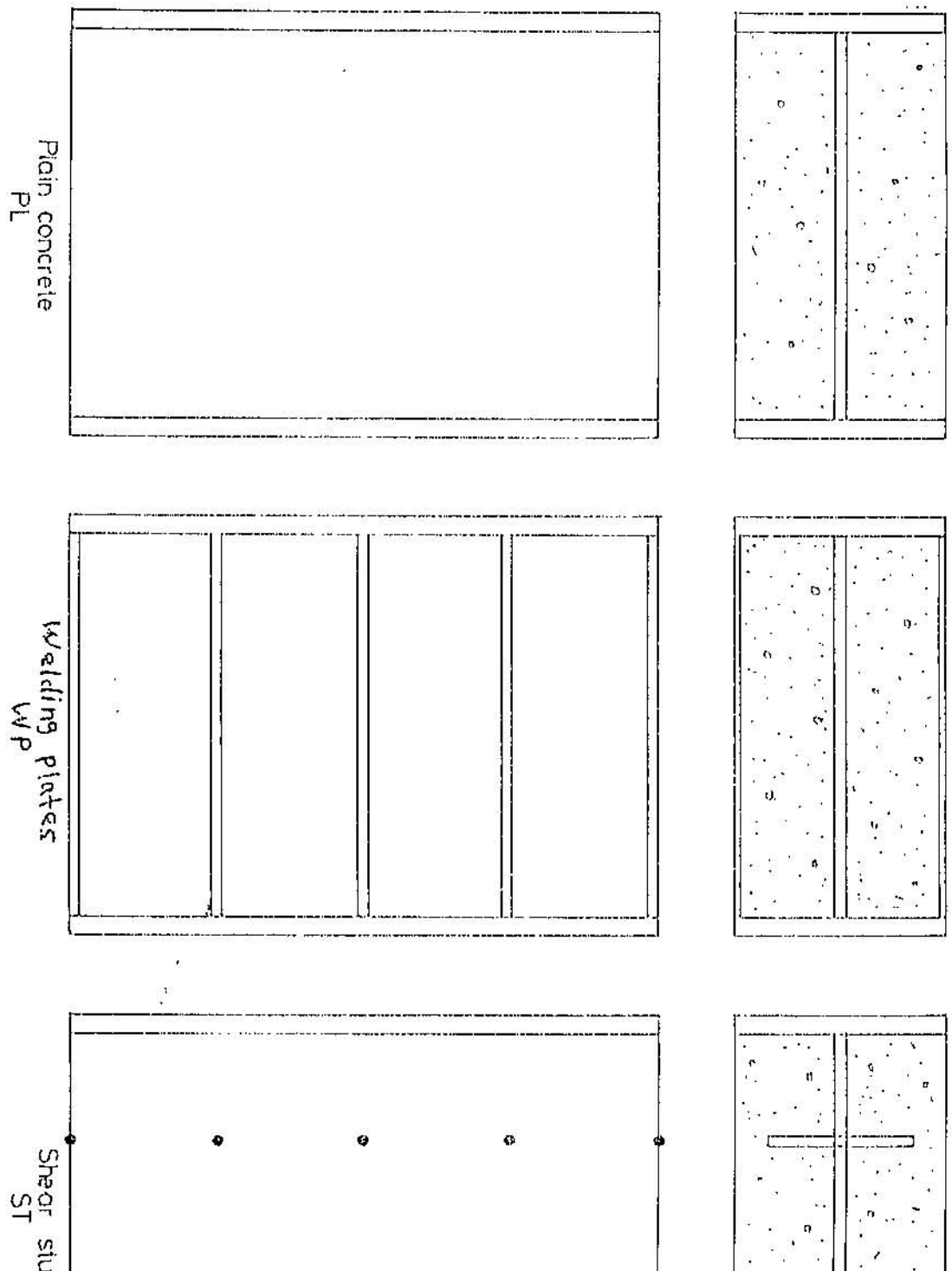

Figure (3.7): Cross sections in the test specimens

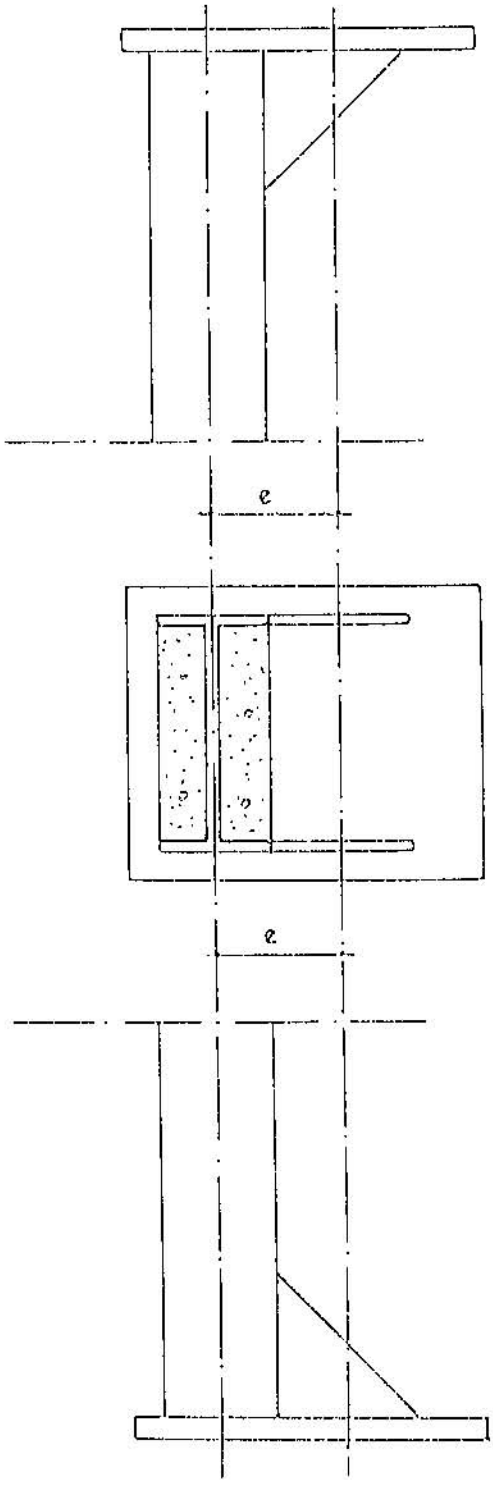

Figure (3.8): Column ends with extended end plates

Semi encased column sections were tested in three groups. As a role, three specimens were tested for the study of a given parameter, the properties of the specimen in each group were made as similar as possible, changing only the factor under consideration.

The first group (consists of three specimens) were tested without any shear connectors, i.e plain concrete only, the second group were cast using shear studs. These shear studs were two rods of 8 mm diameter and 35 mm length, the spacing between the shear studs was uniform and dividing the column into four bays. In the third group, the shear studs were replaced by plates of 20 mm length and a thickness of 3 mm. These plates were welded to connect the tips of the flanges of the IPE section, as shown in Figure [3.7].

3.3.2 Materials

The columns were cast and compacted horizontally, one side at a time. It should be mentioned that casting may be considered as an advantage of the semi-encased composite column, were no shuttering is used.

Concrete mix of 10:15:30/0.5 (cement: sand: aggregate / water cement ratio) with maximum size of 10 mm aggregate (uncrushed river gravel), Ordinary Portland Cement and washed river sand were used.

After casting, all specimens were kept moist by covering the concrete with wet hassian for a few days. Three 150 mm cubes were cast with each column and placed in the damp storage room in the laboratory at 24 hours old and remained their until they were removed for testing.

With respect to steel component of the column, the steel section used was originally 12000 mm long. Five column specimens were fabricated from this length and the remaining part (750 mm) was used to determine the mechanical properties of the steel. Mechanical tests required to determine these properties were carried out at the Royal Scientific Society Laboratories. Material properties together with details of the columns are given in Tables [3.1,3.2], and considering K_1 as 0.83 and 0.67 respectively.

Table (3.1): Details and properties of columns, (K_1 = 0.83).

Column No. and case	e mm	f_y MPa	f_{cu} MPa	steel section B x H mm x mm	Area of steel, A_s , mm^2	Area of concrete A_c , mm^2	concrete cont. factor α_c	Squash load Nu kN	Mu kN.m (5)
1PL(1)	70.	310.	51.6	101.0x202.0	2753.0	17649.0	0.470	1609.3	23.37
2PL	50.	310.	50.9	101.0x201.5	2750.2	17601.3	0.466	1596.2	23.23
3PL	30.	310.	50.1	102.0x202.5	2772.8	17882.2	0.464	1603.2	23.60
1ST(2)	70.	310.	51.6	101.5x202.5	2764.3	17789.5	0.471	1618.8	23.65
2ST	50.	310.	50.9	101.0x202.0	2753.0	17649.0	0.466	1599.0	23.26
3ST	30.	310.	50.1	101.5x203.0	2767.1	17837.4	0.464	1599.5	23.40
1WP(3)	70.	310.	51.6	101.0x202.5	2755.8	17696.7	0.470	1612.2	23.40
2WP	50.	310.	50.9	101.0x202.5	2755.8	17696.7	0.467	1601.9	23.28
3WP	30.	310.	50.1	100.5x203.0	2750.1	17651.4	0.463	1586.5	22.95
1BS(4)	30.	310.	—	102.0x202.0	2770.0	———	———	858.7	14.16

(1)- PL : Plain concrete

(2)- ST : Shear studs

(3)- WP : Battened flanges

(4)- BS : Bare steel

(5)- M_u : Values of ultimate moment of resistance are computed from the derived equations as in Appendix A.

Table (3.2): Details and properties of columns, (K_1 = 0.67).

Column No. and case	e mm	f_y MPa	f_{cu} MPa	steel section B x H mm x mm	Area of steel, A_s ,mm^2	Area of concrete A_c ,mm^2	concrete cont. factor α_c	Squash load Nu kN	Mu kN.m (5)
1PL(1)	70.	310.	51.6	101.0x202.0	2753.0	17649.0	0.417	1463.6	21.65
2PL	50.	310.	50.9	101.0x201.5	2750.2	17601.3	0.413	1452.8	21.53
3PL	30.	310.	50.1	102.0x202.5	2772.8	17882.2	0.411	1459.8	21.87
1ST(2)	70.	310.	51.6	101.5x202.5	2764.3	17789.5	0.418	1472.0	21.88
2ST	50.	310.	50.9	101.0x202.0	2753.0	17649.0	0.414	1455.3	21.55
3ST	30.	310.	50.1	101.5x203.0	2767.1	17837.4	0.411	1456.5	21.68
1WP(3)	70.	310.	51.6	101.0x202.5	2755.8	17696.7	0.417	1466.1	21.67
2WP	50.	310.	50.9	101.0x202.5	2755.8	17696.7	0.414	1457.8	21.57
3WP	30.	310.	50.1	100.5x203.0	2750.1	17651.4	0.410	1445.0	21.27
1BS(4)	30.	310.	—	102.0x202.0	2770.0	——	——	858.7	14.16

(1)- PL : Plain concrete

(2)- ST : Shear studs

(3)- WP : Battened flanges

(4)- BS : Bare steel

(5)- M_u : Values of ultimate moment of resistance are computed from the derived equations as in Appendix A.

3.4 Instrumentation

The columns were instrumented to measure loads, deflections (horizontal & vertical) and strains in concrete as will be described in the following sections.

3.4.1 Load Measurements

All columns were tested under incremental monotonic loading. The applied load was recorded directly from the load indicator of the testing machine discussed in section (3.2) and as shown in Figure [3.1].

3.4.2 Deflection Measurements

Lateral deflections were measured by dial gauges of 0.01 mm precision. One dial gauge was placed at mid height of the column, similar dial gauges were also used to measure displacements and rotations at the column ends, as shown in Figure [3.9].

3.4.3 Strain Measurements

Demec gauges were used to measure strains in concrete. The strains were measured by 4-inch demec gauges, these were located at the mid height of the column as shown in Figure [3.10].

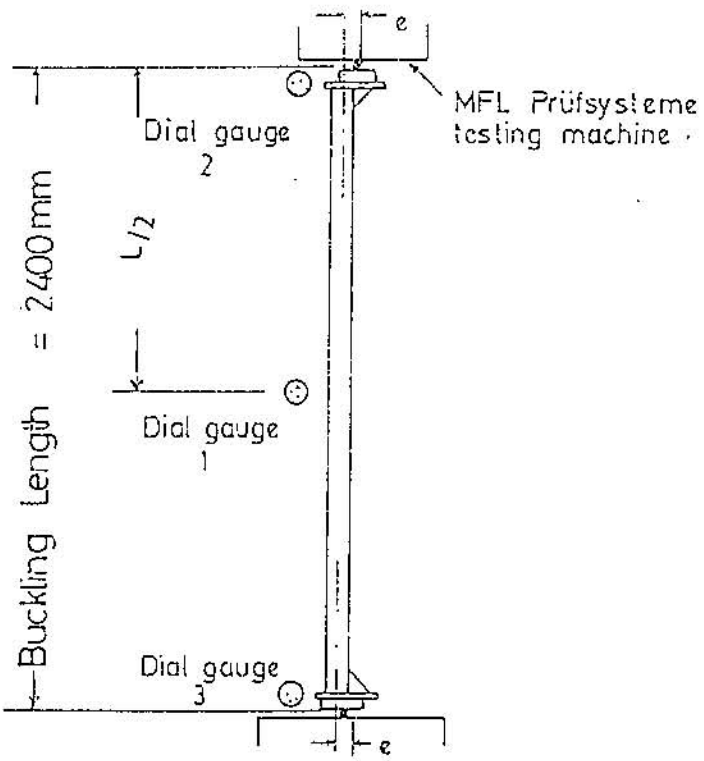

Figure (3.9): Locations of dial gauges

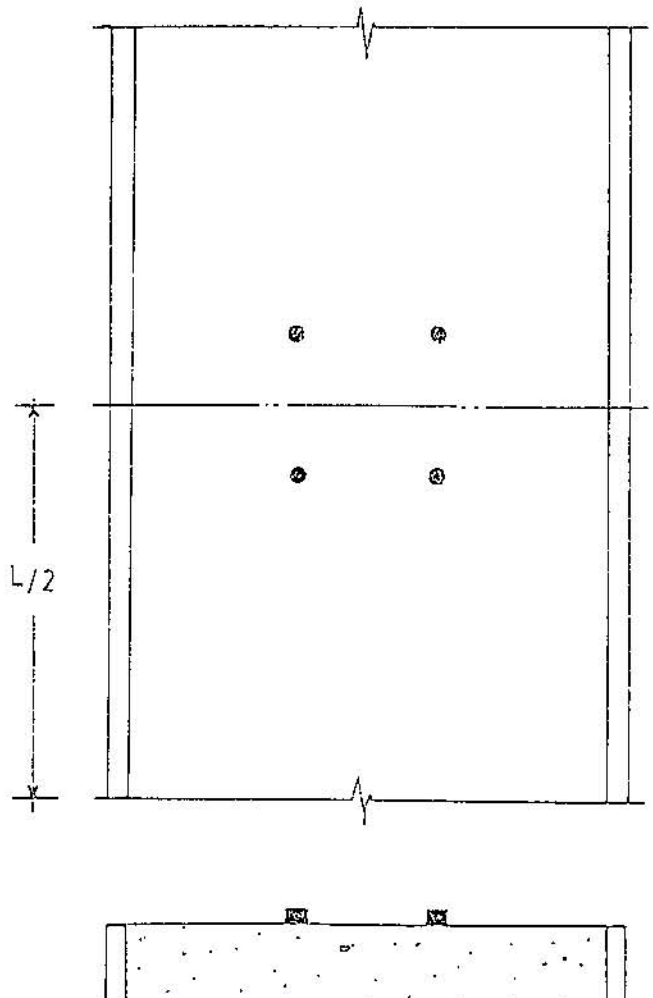

Fgiure (3.10): Locations of demec gauges

3.4.4 Observation of Cracks

The crack growth on the tension side of concrete was also monitored in most tests. This was made possible by the application of white wash to the concrete, so that, the texture of the concrete face would be very smooth and any cracks occurred could be easily noticed.

3.5 Experimental Procedure

The load was applied eccentrically such as to cause bending about the minor axis in single curvature. The end eccentricity ratio was kept constant and equal to one in all columns.

Due to the load capacity of the testing machine, the loads were applied at eccentricities of 30,50 and 70 mm.

When the column specimen was placed in the test rig, a load of 5 kN was applied and then released prior to testing, to insure that no load loss would occur due to relaxation at the column ends.

The load was applied sequentially up to failure, the load increments were 15% of the estimated failure load up to 50% of the failure load, and 7% up to 75% of the failure load and finally increments of 3% were used up to the failure load. The rate of loading was kept constant for all specimens and

equal to 5 kN/minute.

For each specimens, all required measurements and observations were recorded at each load increment.

CHAPTER IV

RESULTS AND DISCUSSION

Tests have been conducted on ten semi-encased composite columns to create data on this type of composite columns.

This chapter presents the data from these tests and discusses the results. The failure loads of the columns are also compared with the ultimate loads predicated by numerical methods.

4.1 Behavior of columns

Some minor crushing of the concrete was observed in columns prior to the ultimate load stage, this took the form of a localized spalling of the surface of the concrete. The amount of spalling was very small compared with the total cross-sectional area of the concrete, and occurred at positions of maximum lateral deflection (mid-height of the column).

The stage of loading which initiates spalling suggests that no such surface spalling would occur in practice, i.e: there is an apparent satisfactory safety margin against spalling of concrete at service loads.

In most tests, white wash was applied to tension side of the concrete, this made the tension cracks clearly visible

during the progress of the test. Tension cracks were developed at loads greater than 70% of the failure load. In most cases, the crack width remains unwidened when the load further increased, but a new hair-width cracks developed at other sections of the tested column.

Local buckling of steel sections was not observed prior to failure, but flakes of steel were noticed. No sign of local separation was observed between the steel and concrete prior to failure which confirms the composite action between the concrete and the steel.

The term 'separation' is used to indicate the movement of a part of the concrete and the flanges of the steel section. The plates which were welded to the flanges of steel sections, remained at their fixed places without any flakes or damage to welding points, which indicate no sign of separation was occurred.

4.2 Failure loads

The maximum loads sustained by the ten columns are summarized in Tables [4.1,4.2], along with the squash loads based on the measured material properties.

Experimental failure loads were plotted against the eccentricity values as shown in Figure [4.1]. The experimental failure loads, N_e, show that no significant difference in

results obtained by columns of plain concrete, columns with shear studs or columns with batten flanges. This confirms the composite action between the steel and the concrete. Furthermore, the present configuration of shear studs and welded plates in this experimental program have no significant effect on the load carrying capacities of the tested columns.

Figure [4.1] shows that the failure loads are decreased when the eccentricity of the applied load increases. The failure loads are decreasing steeply over the small eccentricity values range, after which the failure load decreased at a much slower rate.

For eccentricity of 30 mm, concrete of 50 Mpa strength enhances the strength of the bare steel column of about 70% of the failure load.

Values of failure loads of the tested columns were calculated by the Newmark's numerical integration technique and Column Deflection Curve method, from an analysis developed by Riyalat [12] and Hamdan [15].

In calculating the theoretical failure loads, the material partial safety factors for steel and concrete were taken as unity. Furthermore, the ultimate strain in concrete has taken to be 0.004. The obtained theoretical results are shown in Tables [4.1,4.2] and considering K_1 as 0.83 and 0.67 respectively.

Each set of failure loads, whether obtained experimentally (N_e) or predicated by Newmark's technique (N_n) or CDC (N_c), were normalized with respect to squash load (N_u) as shown in Tables [4.1,4.2]. Interaction curves obtained by Newmark's technique are presented in Figures 4.2 and 4.3, and considering K_1 as 0.83 and 0.67 respectively. These are obtained for end eccentricity ratio equal to one and effective length equal to 2400 mm.

The general consistency between the results obtained by Newmark's technique and CDC method, indicates the reliability of the theoretical computations. Results obtained by the two methods above (as shown in Tables 4.1,4,2) were in good agreement for all columns.

Theoretical values of failure loads, (K_1 = 0.83), are compared with experimental results as shown in Table (4.1). It is evident that the agreement is good and the ratios of N_e/N_t (in Table 4.1) range from 0.96 to 1.05 for 70 mm eccentricity, 0.95 to 1.01 and from 1.01 to 1.06 for 50 mm and for 30 mm eccentricities respectively. Columns 1ST and 2WP are failed at loads less than the predicated theoretical values.

Theoretical values of failure loads, (K_1 = 0.67), are compared with experimental results as shown in Table [4.2]. Ratios of N_e/N_t (in Table 4.2) range from 1.01 to 1.11 for 70 mm eccentricity, 1.0 to 1.07 and from 1.08 to 1.13 for 50 mm and 30 mm eccentricities respectively. More discrepancy is

noticed here for small eccentricity values.

As recognized from Tables [4.1,4.2], failure loads with a value of 0.83 for K_1 are in good agreement with experimental failure loads than that of K_1 equal to 0.67.

The main reason for the differences between N_e and N_t is that the theoretical computation methods are essentially approximate ones. Although, these results verify the basic assumption used in the analysis.

Table (4.1): Column results, (K_1 = 0.83).

Column No. and case	e mm	α_c	N_u kN	Failure Load kN			Load Ratio				
				Experimental N_e	Newmark N_n	CDC N_C	N_e/N_u	N_n/N_u	N_c/N_u	N_e/N_n	N_e/N_c
1PL	70.	0.470	1609.3	210.0	200.1	199.8	0.130	0.124	0.124	1.049	1.051
2PL	50.	0.466	1596.2	251.0	253.3	253.1	0.157	0.159	0.159	0.991	0.992
3PL	30.	0.464	1603.2	364.0	359.6	359.5	0.227	0.224	0.224	1.012	1.013
1ST	70.	0.471	1618.8	193.0	202.0	202.3	0.119	0.125	0.125	0.955	0.954
2ST	50.	0.466	1599.0	255.0	253.6	253.3	0.159	0.159	0.158	1.006	1.007
3ST	30.	0.464	1599.5	378.0	355.6	355.5	0.236	0.222	0.222	1.063	1.063
1WP	70.	0.470	1612.2	200.0	200.4	200.0	0.124	0.124	0.124	0.998	1.000
2WP	50.	0.467	1601.9	240.0	253.9	253.6	0.150	0.159	0.158	0.945	0.946
3WP	30.	0.463	1586.5	365.0	346.8	346.7	0.230	0.219	0.219	1.050	1.053
1BS	30.	——	858.7	215.0	193.4	192.6	0.250	0.225	0.224	1.112	1.116

Table (4.2): Column results, (K_i = 0.67).

Column No. and case	e mm	α_c	N_u kN	Failure Load kN			Load Ratio				
				Experimental N_e	Newmark N_n	CDC N_C	N_e/N_u	N_n/N_u	N_c/N_u	N_e/N_n	N_e/N_c
1PL	70.	0.417	1463.6	210.0	188.8	188.9	0.143	0.129	0.129	1.112	1.112
2PL	50.	0.413	1452.8	251.0	239.9	238.6	0.173	0.165	0.164	1.046	1.052
3PL	30.	0.411	1459.8	364.0	338.0	337.7	0.249	0.232	0.231	1.077	1.078
1ST	70.	0.418	1472.0	193.0	191.6	191.3	0.131	0.130	0.130	1.007	1.009
2ST	50.	0.414	1455.3	255.0	238.9	239.2	0.175	0.164	0.164	1.067	1.066
3ST	30.	0.411	1456.5	378.0	333.8	334.0	0.260	0.229	0.229	1.132	1.132
1WP	70.	0.417	1466.1	200.0	189.0	189.1	0.136	0.129	0.129	1.058	1.057
2WP	50.	0.414	1457.8	240.0	239.2	239.4	0.165	0.164	0.164	1.003	1.003
3WP	30.	0.410	1445.0	365.0	325.9	325.0	0.253	0.226	0.226	1.120	1.120
1BS	30.	——	858.7	215.0	193.4	192.6	0.225	0.225	0.224	1.112	1.116

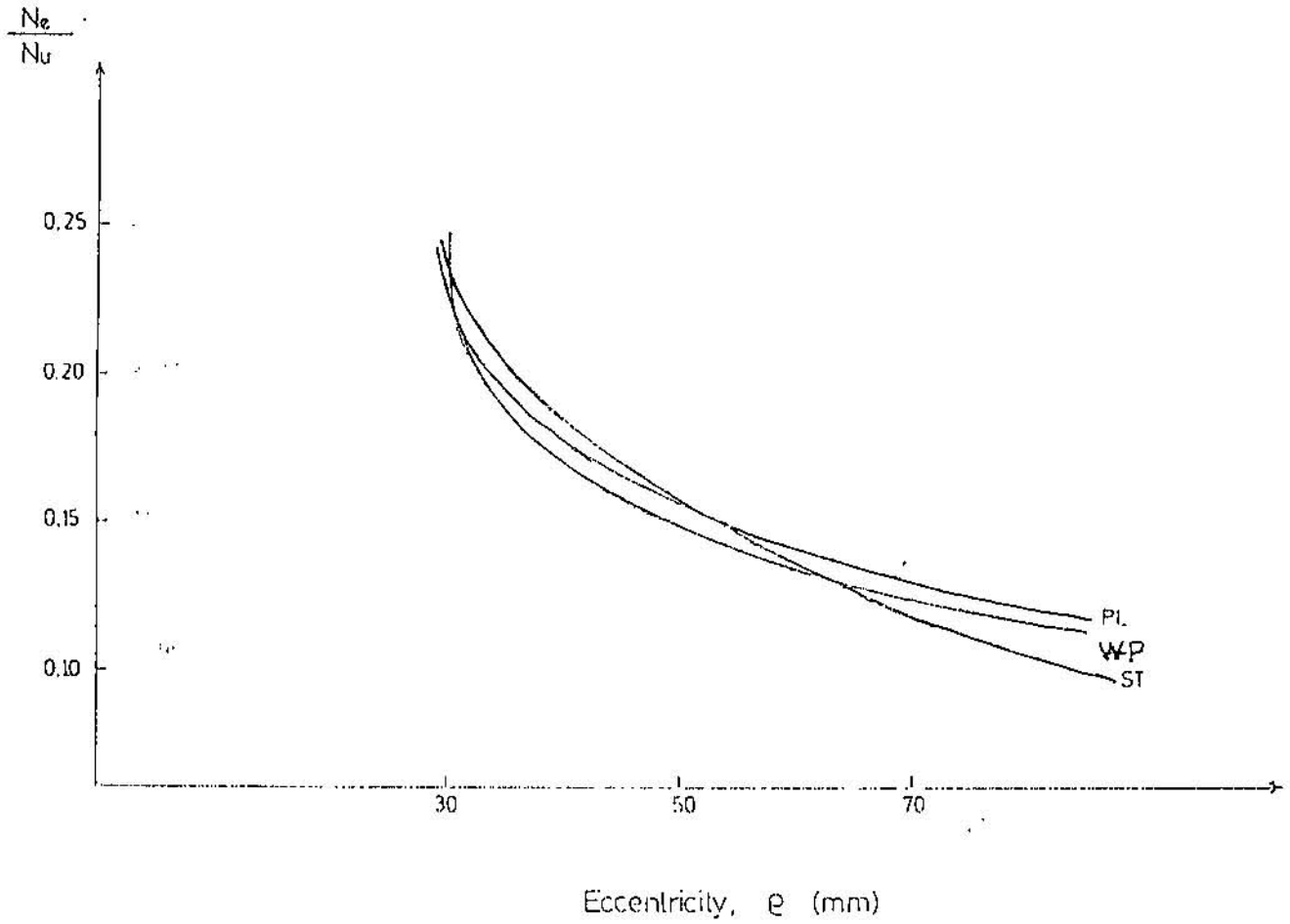

Figure (4.1): Experimental failure loads vs. eccentricity values.

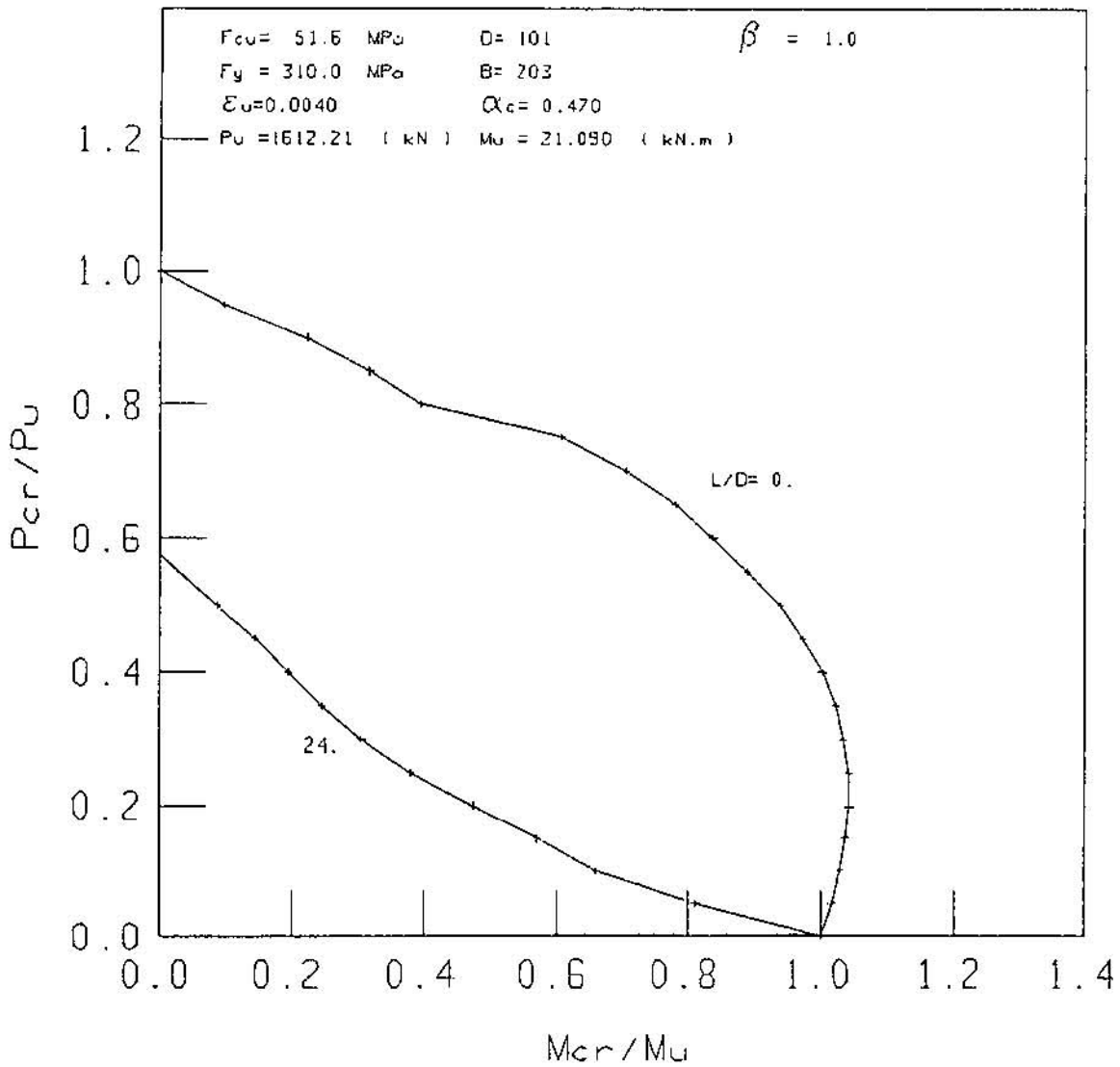

FIG. (4.2) : ULTIMATE STRENGTH INTERACTION CURVES FOR IPE SEMI - ENCASED COLUMN UNDER UNIAXIAL BENDING ABOUT MINOR AXIS

** USING NEWMARK METHOD

$K_1 = 0.83$

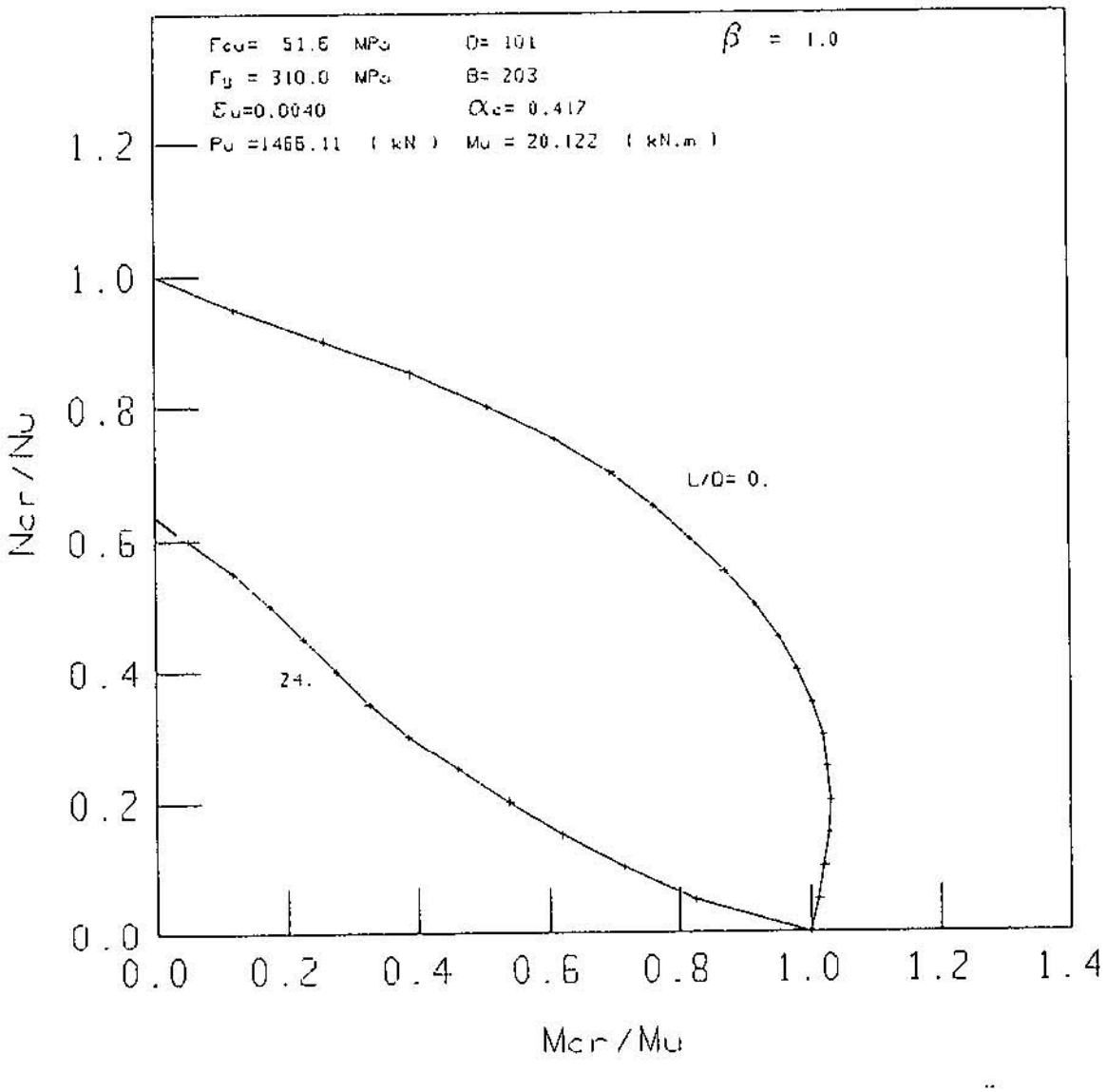

FIG. (4.3) : ULTIMATE STRENGTH INTERACTION CURVES FOR IPE SEMI - ENCASED COLUMN UNDER UNIAXIAL BENDING ABOUT MINOR AXIS

** USING NEWMARK METHOD

$K_1 = 0.67$

4.3 Strains

Typical strain data obtained during the test have been expressed in the form of the load-strain curves shown in Figure (4.4). The strains in concrete were measured only as mentioned in section (3.4.3). Mid-height strains in plane of bending in column 1WP are shown in Figure (4.5).

The maximum recorded strains in compression concrete range from 0.0024 to 0.0038. When compared with theoretical values, the maximum recorded strains were always less than the maximum theoretical values, this is due to to the fact that the experimental values were always at loads slightly lower than the load which caused failure.

Since the steel would have attained its yield stress at strains between 0.0013 and 0.0016, it's clear from Figures 4.4 and 4.5 that the steel flanges yielded at failure, since strains of the above magnitudes were recorded during the testing.

Due to some difficulties in testing, the strain values where measured at two faces only, so the values of neutral axis as shown in Figure [4.5] don't reflect the true behavior of such columns under loading. It would seem that using electrical strain gauges are desirable when measuring the strain values.

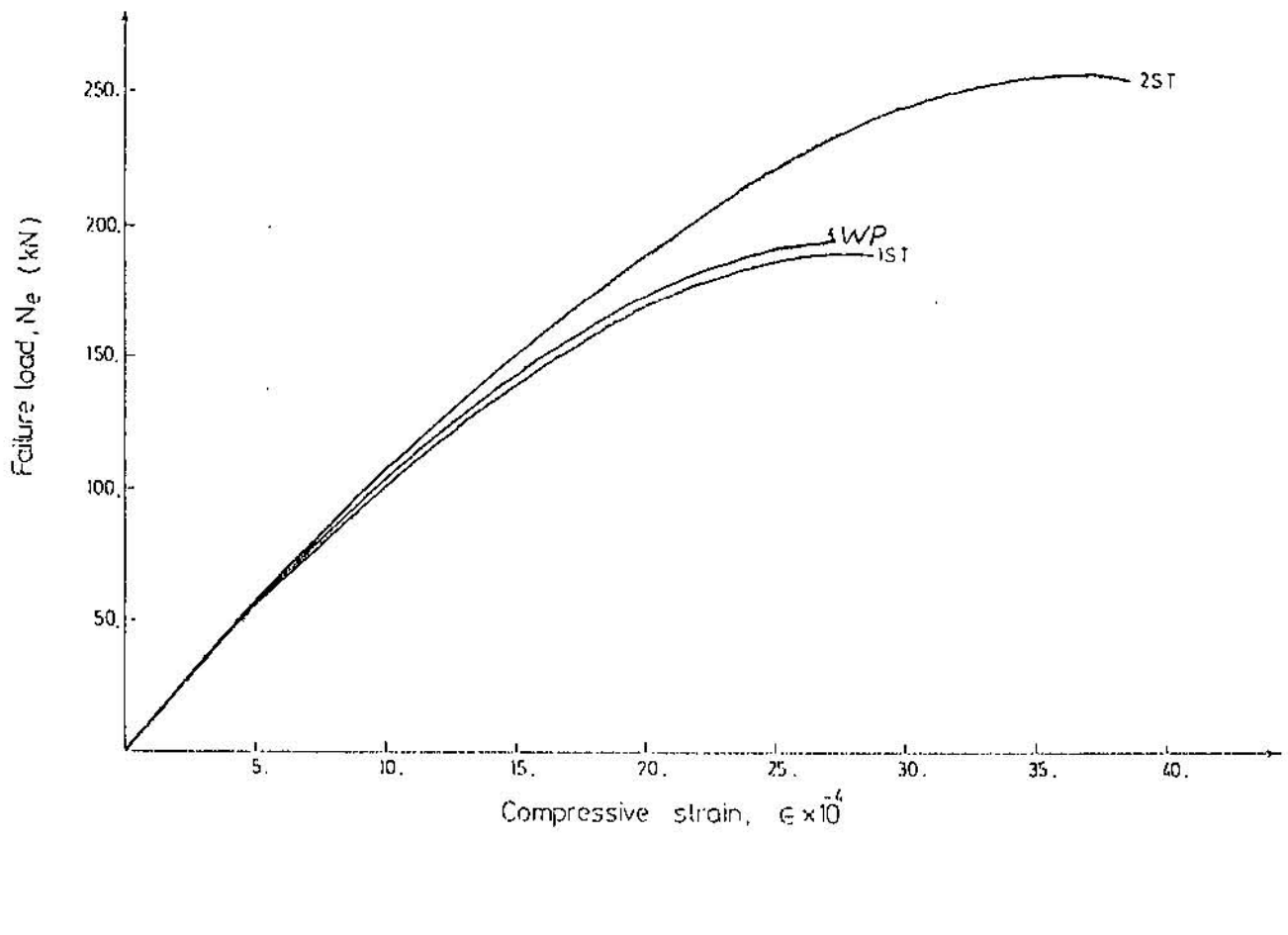

Figure (4.4): Load vs. concrete strain curves for columns 1ST, 2ST and 1WP.

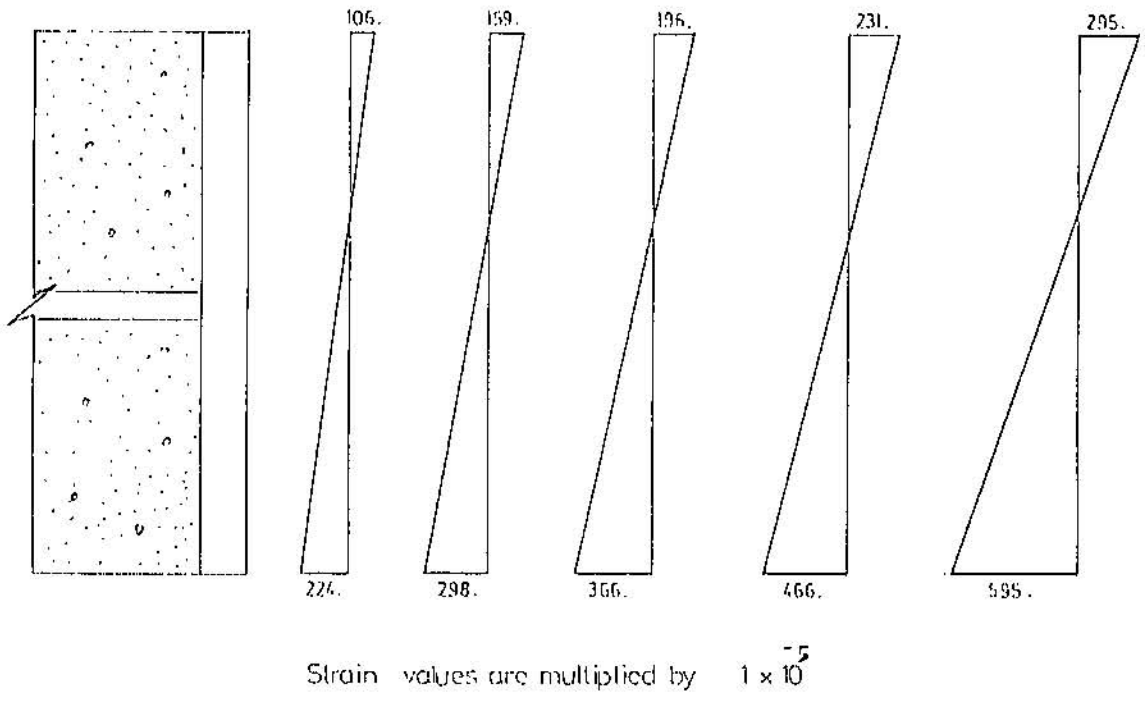

Figure (4.5): Mid-hieght strains in plane of bending for column 1WP.

4.4 Deflections

Deflections relative to minor axis were measured at the mid-height of the columns, and are shown in Figure (4.6). Theoretical values of maximum deflections along with the experimental values are shown in Table (4.3). From these results, the effect of the eccentricity of the applied load can be clearly seen.

The lateral deflections of the tested columns was small until the load on the columns approached the maximum and appreciable increase in deflection is noticed.

For K_1 = 0.83, maximum experimental deflections of columns were less than theoretical values, as shown in Table (4.3). The δ_e/δ_{T1} ratios range from 0.90 to 0.98. Exceptions are columns 2PL, 3WP, and BS, where the ratios were 1.111, 0.742 and 0.397 respectively.

For K_1 = 0.67, maximum experimental deflections of columns were greater than theoretical values for 70 and 50 mm eccentricities. The δ_e/δ_{T2} ratios range from 1.06 to 1.15 for 70 mm eccentricity, and from 1.05 to 1.18 for 50 mm eccentricity. While for 30 mm eccentricity the δ_e/δ_{T2} ratios range from 0.78 to 0.96.

As recognized from deflection results, the value of 0.83 for K_1 seems to be more reasonable to use for the purpose

of comparison with experimental findings.

It is important to mention that the theoretical computations of maximum deflections did not take into account the initial imperfections and residual stresses of the tested columns.

Table (4.3]: Deflection results of the tested columns.

Column No. and case	e_y mm	Maximum Lateral defl. mm Experimental δ_e	theoritical δ_{T1}*	theoritical δ_{T2}**	Deflection ratio δ_e/δ_{T1}	Deflection ratio δ_e/δ_{T2}
1PL	70.	35.10	35.83	30.57	0.980	1.148
2PL	50.	33.50	30.16	28.31	1.111	1.183
3PL	30.	23.70	25.10	24.75	0.944	0.958
1ST	70.	32.90	33.50	31.00	0.982	1.061
2ST	50.	29.30	30.15	27.69	0.972	1.047
3ST	30.	22.70	25.26	24.09	0.899	0.942
1WP	70.	33.30	36.20	30.69	0.920	1.085
2WP	50.	31.80	32.59	27.78	0.976	1.145
3WP	30.	18.90	25.48	24.40	0.742	0.775
1BS	30.	21.90	55.11	55.11	0.397	0.397

* δ_{T1} : Theoretical deflections were calculated using $K_1 = 0.83$

** δ_{T2} : Theoretical deflections were calculated using $K_1 = 0.67$

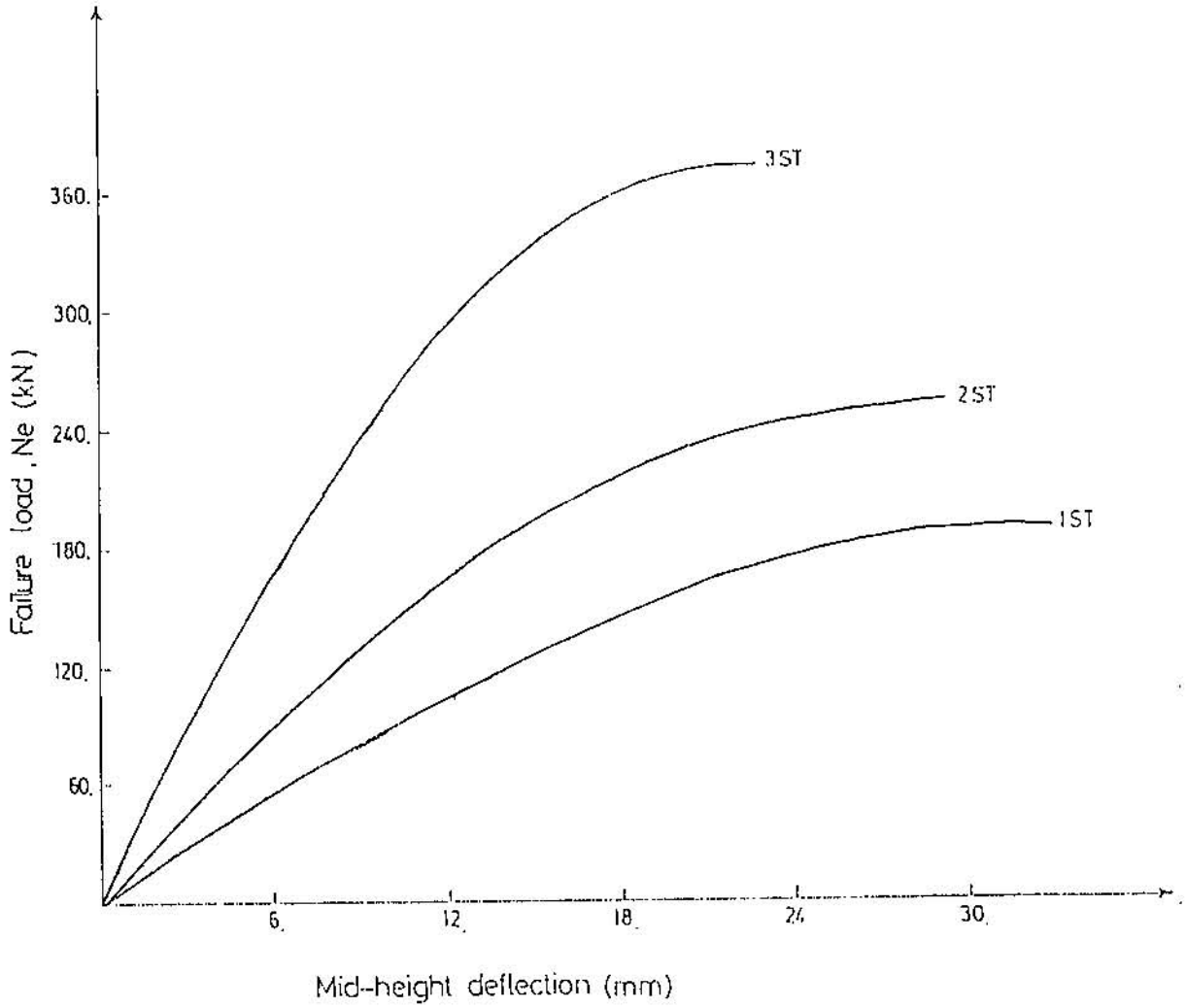

Figure (4.6): Load-deflection curves for columns 1ST, 2ST and 3ST.

CHAPTER V

SUMMARY AND CONCLUSIONS

As a part of the general investigation on the behavior of semi-encased composite columns, experimental and theoretical works were conducted on ten full scale columns. The maximum strength of the tested columns were obtained by deflection methods using Newmark's technique of numerical integration and the Column Deflection Curve method.

The variables studied in this research were the eccentricity of the applied load and the composite action in such column.

From the test results reported in this study, it is seen that the semi-encased composite column behaves as one would expect from a typical composite column.

The following remarks and conclusion can be drawn from this study:

1. The investigation carried out on semi-encased composite column confirmed the composite action between the concrete and the steel section.
2. Omitting the shear connectors and the welded plates has no effect on the load carrying capacity.
3. Experimental and theoretical results indicate that the failure loads decrease as the eccentricity values increase, while the lateral deflections increase.

4. Experimental failure loads compare satisfactory with values predicated by numerical methods. Thus, the test results confirmed the validity of the computational methods used in this study.
5. A value of $K_1 = 0.83$ seems to be reasonable when comparing with experimental results, while, $K_1 = 0.67$ must be used for the design purposes of composite columns in addition to the material partial safety factors.
6. No sign of local buckling and separations between steel and concrete were recognized until failure loads.

Further tests on semi-encased composite columns, using wider range of sectional dimensions, material properties, eccentricities and slenderness ratios seem to be desirable in order to study the general behavior of the semi-encased composite columns and to confirm the analytical findings and validity of computational methods.

Finally, researchs on other aspects, such as details of beam-to-column connections, effect of residual stresses, initial imperfections and the behavior of this composite columns under biaxial bending seem to be necessary.

REFERENCES

1- JONES, R. and RIZK, A.A :An investigation on the behavior of encased steel columns under load". The Structural Engineer, Vol. 41, January 1962, PP 21-33.

2- FABER, O. : "More rational design of cased stanchions". The Structural Engineer, Vol. 34, March 1956, PP 88-109.

3- STEVENS, R. F. : "Encased steel stanchions and BS 449". Journal of the Structural Engineering, ASCE, Vol. 188, Oct. 1959, PP 376-377.

4- BASU, A.K. : "Computation of failure loads of composite columns" Proc. Instn. Civil Engineers, Vol. 36, March 1967, PP 557-578.

5- FURLONG, R. W. : "Design of steel-encased concrete beam-columns". Journal of the structural Division, ASCE, Vol. 1, Jan. 1968, PP 267-281.

6- KNOWLES, R. B. and PARK, R.: "Strength of concrete filled steel tubular columns". Journal of the Structural Division, ASCE, Vol. 12, Dec. 1969, PP 2565-2587.

7- BASU, A.K. and SOMMERVILLE, W. : " Derivation of formula for the design of rectangular composite columns". Proc. Instn. Civil Engineers, Supp. Vol., 1969, PP 233-280.

8- VIRDI, K.S. and DOWLING, P.J. : "The ultimate strength of composite columns in biaxial bending". Proc. Instn. Civil engineers, Vol. 55, 1973, PP 251-272.

9- BS 5400 : "Steel concrete and Composite Bridges; Part 5: Code of practice for design of composite bridges". British Standard Institution, 1979.

10- LITZNER, H.U. and CRISINEL, M. : "Effect of residual stresses on the carrying capacity of battened composite column" . IABSE Proceeding, P- 39/91, 1981, PP 13-30.

11- DUNBERRY, E., LEBLANCE, D. and REDWOOD, G.: "Cross-section strength of concrete-filled HSS columns at simple beam connections". Can. J. Civ. Eng. Vol. 14, 1987, PP 408-417.

12- RIYALAT, S.S. : "Load carrying capacity of battened composite column under major axisbending". M.Sc. Thesis, University of Jordan, 1990.

13- AL-HALLIE, O.A: "Load carrying capacity of battened composite column under minor axis bending". M.Sc. Thesis, University of Jordan, 1990.

14- IRSHEDAT, H. : "Effect of residual stresses on the capacity of battened composite columns under minor axis bending". M. Sc. Thesis, University of Jordan, 1990.

15- HAMDAN, M.A: "Approximate methods for calculating the ultimate strength of composite columns", M.Sc. Thesis, University of Jordan, 1990.

16- SAWALHA, M. "Experimental study of the effect of eccentricity ratio on the ultimate strength of battened composite columns under major axis bending". M.Sc. Thesis, University of Jordan, 1991.

17- ASAD, M. : "Experimental evaluation of the eccentricity ratio effect on the load carrying capacity of battened composite columns under minor axis bending". M. Sc. Thesis, University of Jordan, 1991.

18- HUNAITI, Y. : "Design consideration of Partially Encased Composite Columns". To be Published.

19- European Convention of Constructional Steelwork, (ECCS): "Composite structures". The Constructional Press, 1981, PP 4-25.

20- B S 449 : Part 2. "The use of structural steel in buildings". British Standard Institution, 1959.

21- HUNAITI, Y. : "Composite columns of semi-encased sections". Accepted for Publication in DIRASAT.

APPENDIX A

Derivation of ultimate moment of resistance for semi-encased composite column bending about minor axis

APPENDIX A

The ultimate bending moment, M_u, of a column section is determined by considering equilibrium across a fully plastic section. The calculation of the equilibrium condition is based on the standard practice of assuming rectangular stress blocks in both steel and concrete.

The method of calculating M_u is based on the following assumptions:

1- Area of steel below the neutral axis is stressed in tension to the yield stress, f_y.
2- Area of steel above the neutral axis is stressed in compression to the yield stress, f_y.
3- Area of concrete below the neutral axis is cracked and ignored.
4- Area of concrete above the neutral axis is under a uniform compressive stress, f_c.
5- The flanges of the steel sections have constant thickness.

For a specified value of depth of yielding (d) across the section depth, compression and tension forces are calculated, the ultimate moment of resistance is equal to the sum of moments of tension and compression forces in steel and concrete about mid depth of the section.

In calculating the ultimate moment of resistance of semi-encased composite columns, bending about minor axis, the

following two cases may be investigated [18]:

Case I : The neutral axis lies above the web

Case II: The neutral axis lies within the web.

Minor Axis Bending

CASE I : N.A. Above the web

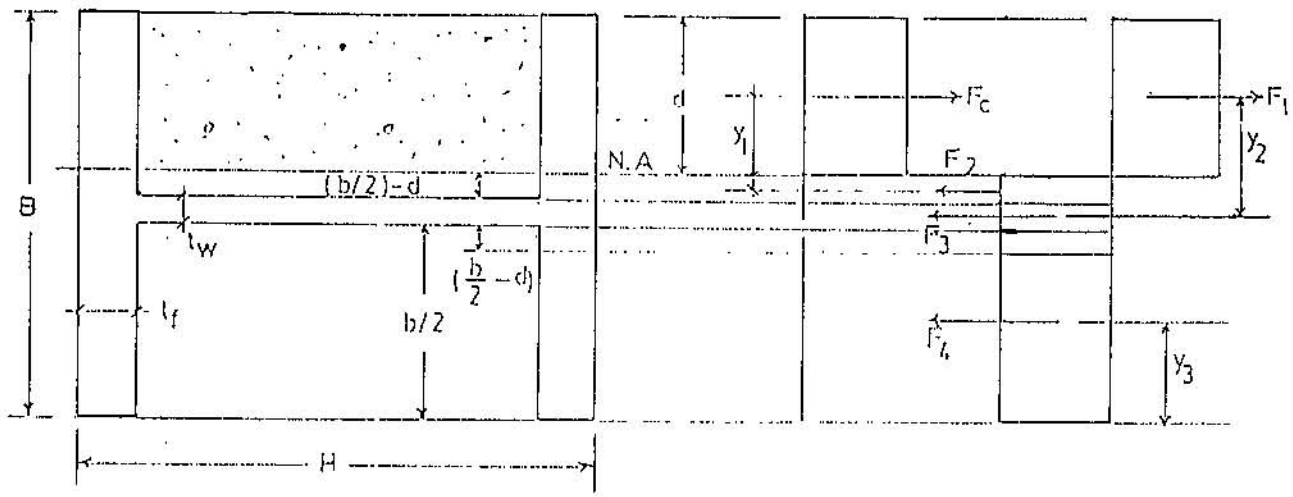

Forces in concrete and steel:

$F_c = d.h.f_c$

$F_1 = 2t_f df_y$

$F_2 = 2(\frac{b}{2} - d)t_f f_y$

$F_3 = Ht_w f_y$

$F_4 = bt_f f_y$

Where: $h = H - 2\,t_f$

To compute depth of N.A.; equate tension to compression forces, which gives:

$F_c + F_1 = F_2 + F_3 + F_4$ OR

$F_c = 2F_2 + F_3$

$$\Longrightarrow d.h.f_c = 2(2\{\frac{b}{2} - d\}t_f.f_y) + Ht_w f_y$$

$$= 2t_f bf_y - 4t_f df_y + Ht_w f_y$$

$$\Longrightarrow d(h.f_c + 4t_f f_y) = (2bt_f + Ht_w)\ f_y$$

OR

$$d = \frac{(2bt_f + Ht_w)\ f_y}{h.f_c + 4t_f f_y} \quad = \frac{\{2(B-t_w)t_f + Ht_w\}f_y}{(H-2t_f)f_c + 4t_f f_y}$$

Also

$$d = \frac{(2Bt_f+(H-2t_f)t_w)f_y}{(H-2t_f)f_c+4t_f f_y}$$

Finally:

$$d = \frac{\{2Bt_f+(H-2t_f)t_w\}f_y}{Hf_c + 2t_f\ (2f_y - f_c)}$$

Force arm:

$$y_1 = \frac{1}{2}\ (\frac{b}{2} - \alpha) + \frac{d}{2} = \frac{b}{4} \qquad (\alpha = d)$$

$$y_2 = \frac{B}{2} - \frac{d}{2} = \frac{1}{2}\ (B-d)$$

$$y_3 = \frac{b}{4}$$

$$\text{Arm of } F_4 = B - y_3 - d/2$$

Ultimate moment of resistance (M_u), could now be computed:

$$M_u = F_2.y_1 + F_3.y_2 + F_4\ (B-\frac{b}{4} - \frac{d}{2})$$

$$M_u = \left\{2(\frac{b}{2} - d)t_f f_y \frac{b}{4}\right\} + \left\{Ht_w f_y(\frac{1}{2}(B-d))\right\} + \left\{bt_f f_y(B-\frac{b}{4} - \frac{d}{2})\right\}$$

$$M_u = \left(\frac{b^2}{4} t_f f_y - \frac{2dbt_f f_y}{4}\right) + \left(\frac{BHt_w f_y}{2} - \frac{dHt_w f_y}{2}\right)$$

$$+ \left(bt_f f_y B - \frac{b^2}{4} t_f f_y - \frac{bd}{2} t_f f_y\right)$$

$$M_u = -2\frac{bdt_f f_y}{2} + \frac{BHt_w f_y}{2} - \frac{dHt_w f_y}{2} + bt_f f_y B$$

$$M_u = \left(\frac{BHt_w f_y}{2} - \frac{dHt_w f_y}{2}\right) + (bt_f f_y B - bdt_f f_y)$$

$$M_u = \frac{1}{2} HT_w f_y (B-d) + bt_f f_y (B-d)$$

$$M_u = (B-d)\left\{\frac{1}{2}\left(HT_w + 2bt_f\right)\right\} f_y$$

$$M_u = \frac{1}{2}\{HT_w + 2bt_f\}(B-d) f_y$$

but $HT_w + 2bt_f = A_s$ (Area of steel section)

Therefore;

$$M_u = \frac{1}{2} A_s (B-d) f_y$$

For bare steel section : the plastic moment is M_p

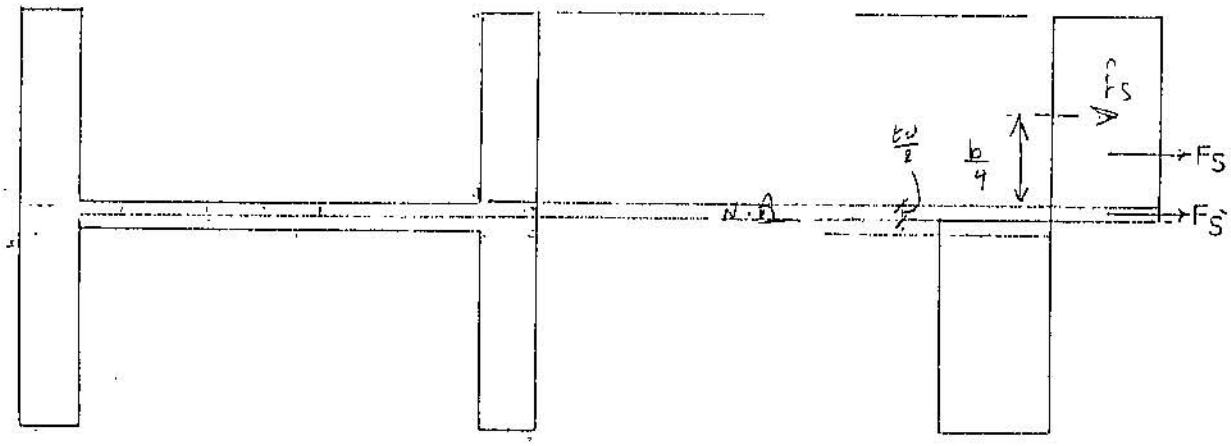

$$F_s = 2t_f \frac{b}{2} f_y = t_f b f_y$$

$$F_s' = \frac{t_w}{2} H f_y$$

$$M_p = 2\left[F_s\left(\frac{b}{4} + \frac{t_w}{2}\right) + F_s' \frac{t_w}{4} \right]$$

$$M_p = 2\left[F_s\left(\frac{b}{4} + \frac{t_w}{2}\right) + F_s'\left(\frac{t_w}{4}\right)\right]$$

$$= 2\left[t_f b f_y\left(\frac{b}{4}+\frac{t_w}{2}\right)+\frac{t_w}{2} H \left(\frac{t_w}{4}\right) f_y\right]$$

$$M_p = \left[t_f b\left(\frac{b}{2} + t_w\right) + \frac{H t_w}{4}\right] f_y$$

$$= \left[\frac{t_f b^2}{2} + t_f b t_w + \frac{H t_w^2}{4}\right] f_y$$

$$= \left[t_f b^2 + 2 t_f b t_w + \frac{H t_w^2}{2}\right] \frac{f_y}{2}$$

$$= \left[t_f b^2 + t_f b t_w + \frac{t_w}{2} (2 t_f b + H t_w)\right] \frac{f_y}{2}$$

where :

$$2 t_f b + H t_w = A_s \quad \text{(Area of steel section)}$$

$$b + t_w = B$$

$$b = B - t_w$$

$$M_p = \left[t_f b \left(\frac{b + t_w}{2}\right) + \frac{t_w}{4} A_s\right] f_y$$

$$M_p = \left[B t_f \left(\frac{B - t_w}{2}\right) + \frac{t_w}{4} A_s\right] f_y$$

$$M_p = Z_p f_y$$

Where:

M_p : Plastic bending moment for bare steel section.

An approximation may be tried by computers to check the largest number of sections:

$$M_u = M_p + 0.1 A_c B f_c$$

This approximation assumed N.A. to be in web.

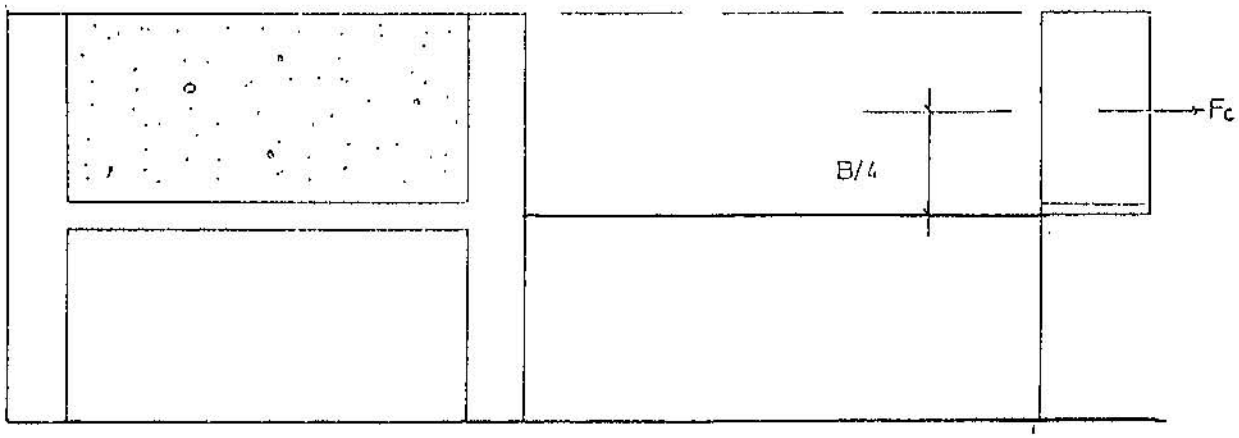

Minor Axis Bending

Case II: N.A in web

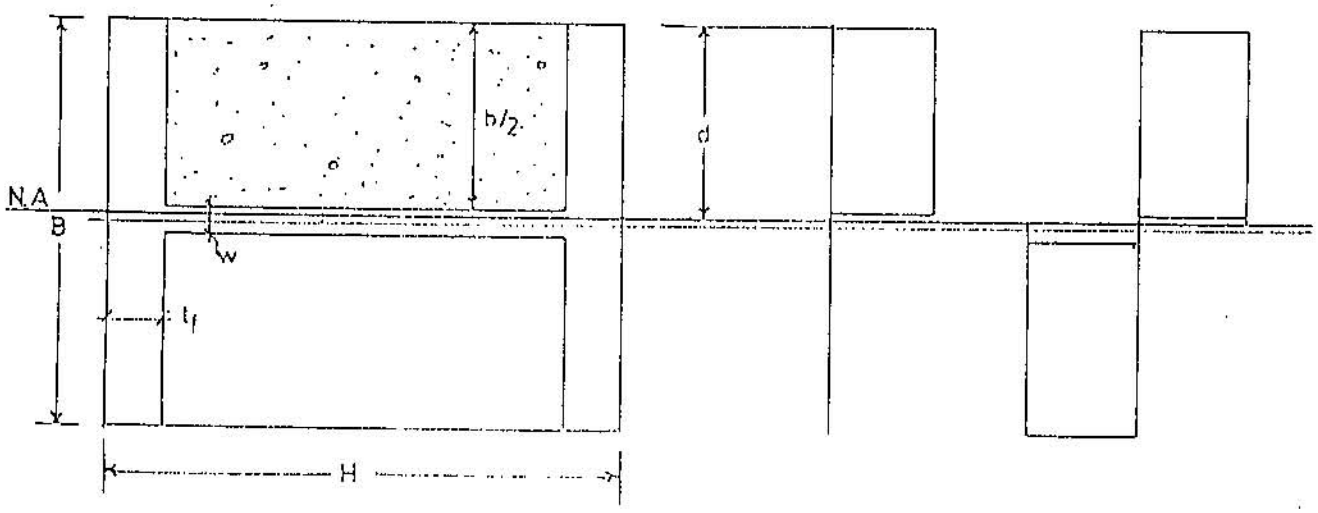

To compute depth of neutral axis:

$$F_c + F_2 = F_3$$

From which

$$\frac{1}{2} A_c f_c + (d-\frac{b}{2}) Hf_y = \left\{ t_w - (d-\frac{b}{2}) \right\} Hf_y$$

$$\frac{1}{2} A_c f_c + (d-\frac{b}{2}) Hf_y = t_w Hf_y - (d-\frac{b}{2}) Hf_y$$

$$2\,(d-\frac{b}{2}) Hf_y = t_w Hf_y - \frac{1}{2} A_c f_c$$

$$2(2dHf_y - bHf_y) = 2(t_w Hf_y - \frac{1}{2} A_c f_c)$$

$$4dHf_y = 2\,H\,f_y\,(b + t_w) - A_c f_c$$

where:

$A_c = BH - A_s$

$B = b + t_w$

from which

$$4\,dHf_y = 2f_yBH - A_cf_c$$
$$= 2f_yBH - BHf_c + A_sf_c$$
$$= BH\,(2f_y - f_c) + A_sf_c$$

OR

$$d = \frac{1}{4f_y}\left\{B(2f_y - f_c) + \frac{A_s}{H}\,f_c\right\}$$

AND

$$M_u = \frac{1}{4}\,f_y\left[4dH\left(\frac{b}{2} - d\right) + t_wH\,(2t_w + b) + 2bt_f(B + t_w)\right]$$

"الأعمدة المركبة ذات المقاطع شبه المكسوة"

الملخص

لقد جرت العادة عند انشاء المباني المكونة من هياكل معدنية ، أن يتم تغليف الاعمدة بالخرسانة لحمايتها من تأثير الحرائق ، ولكن منذ عام ١٩٥٠م ، بدأ الباحثون بدراسة اعتبار الخرسانة كعنصر إنشائي في مقاومة الأحمال ، إضافة الى المقطع المعدني المستخدم في الاعمدة . وبذلك أصبح شائعاً استخدام اعمدة مزكبة من المعدن والخرسانة عند تنفيذ وإنشاء المباني .

في هذا البحث ، تم دراسة قوة التحمل للأعمدة المركبة ذات المقاطع شبه المكسوة المقترحة حديثاً ، وتصرف هذه الاعمدة خلال عملية التحميل .

لقد تم اعداد عشرة اعمدة بمقطع (١٠٠ × ٢٠٠ ملم) وطول ٢٤٠٠ مم ، ثابتين لأغراض المقارنة، وجرى فحصها بواسطة ثلاثة قيم مختلفة للامركزية الحمل (Eccentricity of loading)، في مختبر الانشاءات الثقيلة بقسم الهندسة المدنية في الجامعة الاردنية.

414691

وبدراسة النتائج المخبرية ، وبمقارنتها مع النتائج النظرية والتي تم حسابها بواسطة طريقتين تقريبيتين هما (Newmark's technique and CDC method) تبين امكانية استعمال هذا المقطع عملياً .